Research Square

Preprints are preliminary reports that have not undergone peer review.
They should not be considered conclusive, used to inform clinical practice,
or referenced by the media as validated information.

Quantification of uncertainties associated with lumped and spatially explicit representations of small and medium reservoirs in a hydrological model for flood simulations

Elanchezhiyan Duraisekaran

elanchez08@gmail.com

Indian Institute of Technology Madras https://orcid.org/0000-0002-3363-0186

Krushil Modi

Indian Institute of Technology Madras

Arun Rajasekaran Sankarbalaji

Indian Institute of Technology Madras

Balaji Narasimhan

Indian Institute of Technology Madras https://orcid.org/0000-0003-2609-9320

Research Article

Keywords: Small and medium reservoirs (SMRs), floods, model structure, variance decomposition, HEC-HMS

Posted Date: April 16th, 2026

DOI: https://doi.org/10.21203/rs.3.rs-9142255/v1

License: This work is licensed under a Creative Commons Attribution 4.0 International License. Read Full License

Quantification of uncertainties associated with lumped and spatially explicit representations of small and medium reservoirs in a hydrological model for flood simulations

Elanchezhiyan Duraisekaran, Krushil Modi, Arun Rajasekaran Sankarbalaji, and Balaji Narasimhan*

Department of Civil Engineering, Indian Institute of Technology Madras.

Elanchezhiyan Duraisekaran – ORCID ID - 0000-0002-3363-0186 (Elanchezhiyan Duraisekaran (0000-0002-3363-0186) - ORCID)

Arun Rajasekaran Sankarbalaji – ORCID ID - 0009-0002-0173-114X (Arun Rajasekaran Sankarbalaji (0009-0002-0173-114X) - ORCID)

***Corresponding Author**: Balaji Narasimhan, Department of Civil Engineering, Indian Institute of Technology Madras, Chennai, 600036, India.

ORCID ID - 0000-0003-2609-9320 (Balaji Narasimhan (0000-0003-2609-9320) - ORCID)

Email: nbalaji@civil.iitm.ac.in

Abstract

Small and medium reservoirs (SMRs) play a crucial role in regulating flood flows. However, the uncertainty associated with SMR representation for flood simulations has not been investigated. More importantly, the differentiation of model structure and parameter uncertainty associated with their representation has not been widely studied. Therefore, this research proposes a methodology to quantify the model structure and parameter uncertainties associated with the lumped and spatial explicit representation of SMRs in flood simulations. Four different model configurations were considered – without SMRs (S1), representing both cascade SMRs (CAS) and catchment outlet SMRs (COS) as lumped "surface storage" (S2), representing COS as spatially explicit "reservoirs" (S3), and CAS as "surface storage" and COS as "reservoirs" (S4). The Soil Moisture Accounting (SMA) method in Hydrologic Engineering Center – Hydrologic Modeling System (HEC-HMS) was used to simulate using a set of parameters generated by Latin hypercube sampling (LHC). The variance decomposition technique combined with the bootstrapping method was used to quantify the model structure and parametric uncertainties. The developed methodology was applied to the upstream of the Chembarambakkam reservoir in southern India. The results indicated that lumped representation (S2) contributes to the parametric uncertainty. However, when all four configurations were considered, the proportion of model variance was $86.86 \pm 2.37\%$ very much higher than the parametric variance of $11.88 \pm 2.27\%$. Further, the representation of COS as "reservoirs" ensured an increase in the p-factor from 0.078 for S1 to 0.449 for S3. Overall, the representation of COS as "reservoirs" is necessary for reducing the uncertainty of hydrological flood simulations.

Keywords: Small and medium reservoirs (SMRs), floods, model structure, variance decomposition, HEC-HMS.

1. Introduction

Global flood vulnerability data between 2005 and 2020 suggest that Asia and Europe have regions with the highest flood vulnerability (Duan et al. 2022). Empirical data-based studies conclude that reservoir regulation can affect flood characteristics both at the local scale and the regional scale (Brunner 2021). The degree of regulation through dams has been high in parts of Asia (Han et al. 2024). In this context, the role of large reservoirs (storage capacity greater than 100 Mm^3) on floods has been studied by incorporating reservoir operation in global flood models (Hanazaki et al. 2022). Under future climate change projections, dams can help in reducing the number of people exposed to floods (Boulange et al. 2021). In this regard, the study of the impact of small and medium reservoirs (SMRs) on flood moderation and water conservation has been of recent interest. Pi et al., (2022) mapped more than 3.4 million lakes after partitioning the global lakes into small (<1 km^2) and medium (1–100 km^2) reservoirs. Donchyts et al., (2022) identified and monitored the state of 71,208 SMRs with sizes varying from 0.01 to 100 km^2 and concluded that observation of these reservoirs can help in issuing flood early warning. From the review of the impact of small reservoirs with a storage capacity less than 1 Mm^3, Habets et al., (2018) found that these reservoirs reduce mean annual discharge between 5% and 22%. The degree of regulation defined by the ratio of the cumulative storage capacities of several reservoirs to the annual streamflow volume is higher for many medium reservoirs (1 to 100 Mm^3) upstream, when compared to a single large reservoir downstream (Spinti et al. 2023). However, in hydrologic modeling of river basins for evolving flood management plans, typically only large reservoirs are considered (Sun et al. 2023), while the role of SMRs in flood simulations has not been widely studied. This may introduce considerable uncertainties in semi-arid regions, typically characterized by many manmade storage structures for water conservation. This is mainly because of the lack of information on the hydraulic and discharge characteristics and the absence of monitoring infrastructure for the

storage of these SMRs on a regular basis. Hence, this research focuses on the representation of SMRs in a hydrological model for flood simulations.

Different methods have been proposed to represent SMRs in hydrological models. A comparison of flows with SMRs (lumped approach) and without SMRs was conducted for a portion of the Salivagu watershed using Soil and Water Assessment Tool (SWAT), and the results showed an overestimation of flows when SMRs were not considered (Ramabrahmam et al. 2021). The reservoir module of SWAT (spatially explicit representation) could not be used to represent the 74 SMRs in the Chongyang River Basin (4,853 km^2) and 61 SMRs in the Xixi River Basin (2,466 km^2), due to a lack of data on a large number of SMRs (Yan et al. 2023). Spatio-temporal variation of water surface area was extracted using Sentinel-2 to parameterize SMRs (spatially explicit approach) in SWAT+ to improve the accuracy of hydrologic simulations (Mahmoodi et al. 2024). Considering the role of SMRs in flood moderation, Perera et al., (2020) studied the Alakola ara SMR cascade in Sri Lanka using the Hydrologic Engineering Center – Hydrologic Modeling System (HEC-HMS) by representing SMRs as "reservoirs" (spatially explicit approach). The results concluded that the existence of bunds in SMRs increases the robustness to flood inflows because of the routing mechanism. Devi et al., (2020) stated that the dredging of SMRs (lumped representation) can compensate for the increase in flooding due to urbanization for 1 in 50-year floods for the Adyar subbasin using HEC-HMS. Overall, these studies highlight that while SWAT has been used to evaluate the impact of SMRs on long-term water resources planning and management, HEC-HMS is commonly applied for flood simulations. In addition, both SWAT and HEC-HMS offer lumped and spatially explicit approaches for the representation of SMRs. However, the studies have failed to address the uncertainty associated with the representation of SMRs in hydrological models.

In this context, a limited number of studies have investigated the model structure uncertainty associated with the representation of SMRs. Rabelo et al., (2021) considered the impact of representation of SMRs in SWAT using lumped approaches and spatially explicit approaches in the Conceicao River catchment, Brazil, for understanding the hydrology of catchments in dryland areas. Subsequently, Rabelo et al., (2022) investigated the impact of increasing the density of SMRs on streamflow. Colombo et al., (2024) studied the influence of representation of SMRs – a) no small reservoirs, b) small reservoirs alone, c) strategic reservoirs alone, d) combination of strategic and small reservoirs on the Banabuiu river watershed using Water Availability in Semi-Arid environments-SEDiments (WASA-SED) model on the propagation of hydrological drought. Sankarbalaji et al., (2025) used SWAT to conclude that the representation of SMRs reduced the uncertainty in hydrologic model parameters, resulting in improved confidence bounds in the estimation of water yield for better water resources planning and management. However, the literature remains scant on quantifying the uncertainty due to the spatial and lumped representation of SMRs in a hydrological model.

Uncertainty quantification in hydrological models is commonly addressed using two statistical frameworks: Bayesian approaches and frequentist approaches. The key difference between these approaches lies in the treatment of model parameters and the use of prior information. Pappenberger et al., (2006) developed a decision tree for selecting the method for uncertainty analysis which suggests an informal Bayesian method namely Generalized Likelihood Uncertainty Estimation (GLUE) when model does not have a long run time. In Soil Water Assessment Tool – Calibration and Uncertainty Program (SWAT-CUP), GLUE has been used along with Sequential Uncertainty Fitting (SUFI2) (Abbaspour 2015). Mousavi et al., (2012) implemented the SUFI2 technique for event-based flood simulation studies in the HEC-HMS model. However, a major limitation of generalized likelihood measures is that they do not provide a rigorous framework for comprehensive uncertainty quantification in hydrological

models (Gupta and Govindaraju 2023). In the frequentist approach, model parameters are treated as fixed but unknown quantities. To differentiate model structure and parameter uncertainty, the same set of parameters is applied across all model configurations. Under this setup, the contribution of model structure and parameter uncertainty to the total uncertainty can be quantified using variance decomposition. The variance decomposition technique was applied in SWAT model to find the contribution of parameter uncertainty as a percentage of total uncertainty for streamflow simulation (Datta and Bolisetti 2013). Topmodel was used along with variance decomposition to the quantify the uncertainty associated with hydrological model spatial discretization and baseflow segmentation (Xu and Yan 2022). Variance decomposition has also been applied to quantify uncertainty related with hydrological models, climate models and extreme value distributions (Núñez Mejía et al. 2023) and also used to decompose the uncertainties involved in the estimation of runoff and total nitrogen (Han et al. 2025). Hence, there is a need to use the same set of parameters across the model structures and use the variance decomposition approach to quantify the model structure and parameter uncertainty associated with the representation of SMRs for flood simulations.

From the literature reviewed, it is evident that SMRs play a crucial role in both drought and flood mitigation. Therefore, it is necessary to incorporate the SMRs in hydrological models for flood simulations. While some of the flood modeling studies represent the SMRs as lumped storages (Devi et al. 2020), others adopt a spatially explicit approach (Perera et al. 2020). Although the uncertainty associated with the representation of SMRs (model structure) for water resources planning has been studied (Rabelo et al. 2021; Colombo et al. 2024), there remains a gap in understanding this uncertainty, specifically in hydrological models for flood simulations. Furthermore, studies have not explored the model structure and parameter uncertainty associated with the representation of SMRs in hydrological models. Therefore, the objective of the research is to evaluate the hydrologic model performance due to the model

structure uncertainty associated with the representation of small and medium reservoirs (SMRs) for flood simulations. The novelty of the research is that a methodology is developed to quantify the model structure and parameter uncertainty associated with the representation of SMRs in a hydrological model for flood simulations.

2. Methodology

2.1 Overview

The research is focused on studying the impact of the representation of SMRs on the hydrologic model performance for flood simulations. A methodology is developed to quantify the uncertainty due to the spatial and lumped representation of SMRs in hydrologic models. The Hydrologic Engineering Center – Hydrologic Modeling System (HEC-HMS) is used for this purpose. The flowchart of the methodology adopted for the study is presented in Figure 1.

The Digital Elevation Model (DEM) and location of SMRs are used for the delineation of subbasins in HEC-HMS. The Soil Moisture Accounting (SMA) method was used as the loss method in HEC-HMS for continuous simulation. Landuse/landcover (LULC), DEM, and soil data were used for the SMA loss model parameterization. Four different configurations of SMRs were considered in the study. The SMA model was set up using the input rainfall data for each of the four different configurations. A sensitivity analysis was carried out using a one-at-a-time (OAT) approach independently for each of the four configurations. The uniform prior distribution was assumed for the parameters. Latin hypercube sampling (LHC) was used to generate a set of parameters. The four different model setups were simulated independently using the generated set of LHC parameters as a continuous simulation. With the help of the results from the continuous simulations carried out, the variance decomposition technique combined with the bootstrapping method was used to quantify the model structure and parametric uncertainties associated with the representation of SMRs. Finally, the calibration

and the validation of the four different model configurations were done. Each of the components of the methodology is elaborated in the subsequent sections.

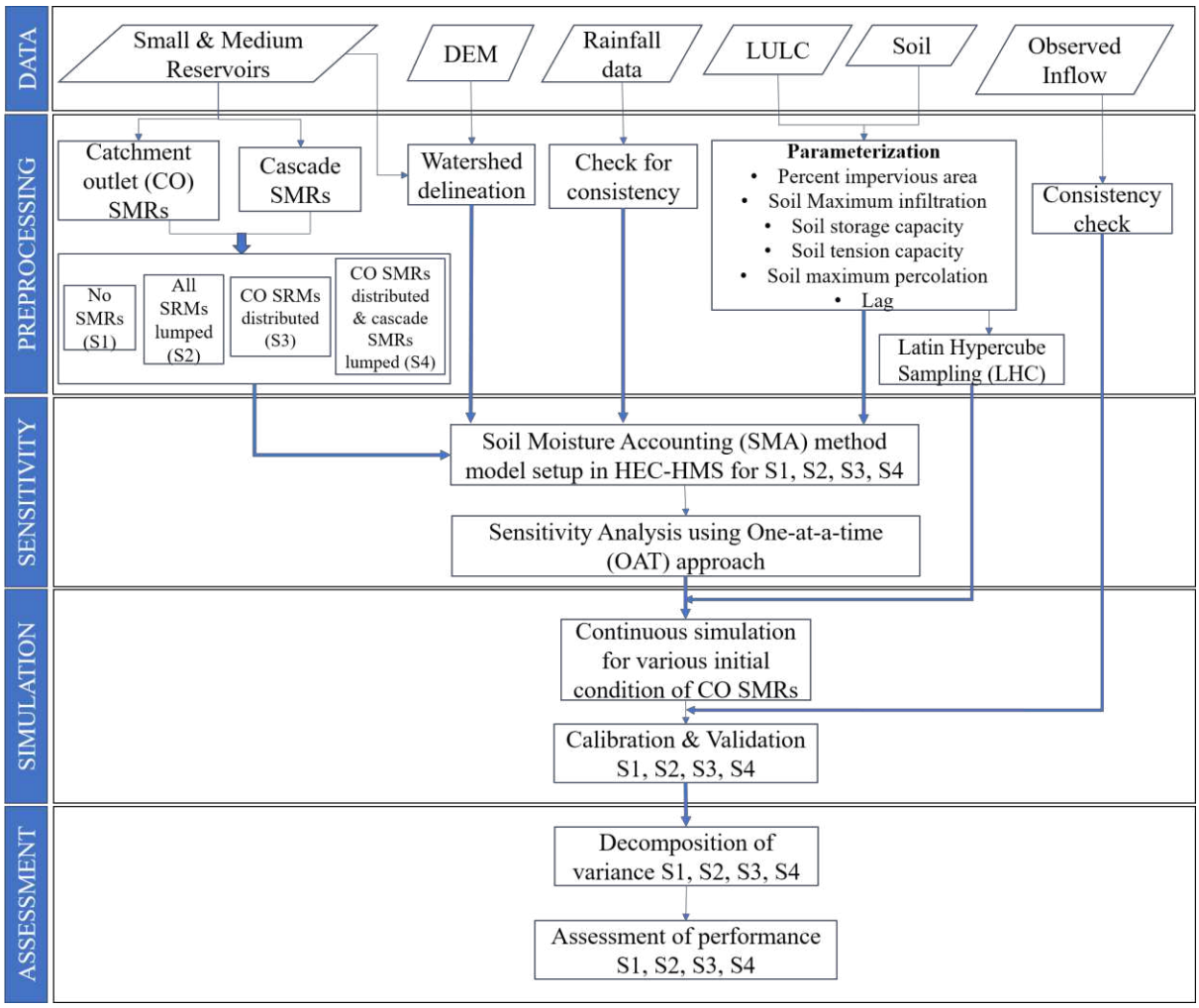


Figure 1. Overview of the methodology adopted for the study

2.2 Hydrological modeling using HEC-HMS

The hydrological modeling was done using the Hydrologic Engineering Center – Hydrologic Modeling System (HEC-HMS). The Soil Moisture Accounting (SMA) method was used as the loss method. The SMA consists of canopy storage, surface storage, and soil storage. Each storage is governed by mass balance. The precipitation falling on the canopy storage can undergo evapotranspiration. The precipitation falling on the ground reaches surface storage, and part of it infiltrates into the ground. After the surface storage fills up, it becomes surface

runoff. The infiltrated amount goes first to the soil upper zone storage and then to the soil tension zone storage. Evapotranspiration can occur from both soil layers. The water from the soil layers can reach the soil storage. After filling up the soil layers, water moves to the groundwater storage. Thus, the SMA method takes care of the interception loss, surface depression loss, and soil storage. The hydrologic model was lumped at the subbasin scale.

Fleming and Neary (2004) discussed the parameterization of the SMA method in the HEC-HMS model using a geographic information system (GIS) for 2424 km^2 of the Dale Hollow watershed and suggested the use of multiparameter sets for improved model performance. Azmat et al., (2017) found that the SMA loss method performed better than the Deficit and Constant loss method for continuous simulation of the Jhelum River catchment, and was able to reproduce the rapid streamflow peaks better. From the detailed literature review, it was suggested that the SMA method was the most widely used and preferred method for continuous modeling in HEC-HMS (Sahu et al. 2023; Odey and Cho 2025).

2.3 Representation of SMRs in HEC-HMS

Two representations of SMRs in HEC-HMS were discussed in the literature. One approach is the lumped approach, where SMRs are represented as “surface storage”, assumed to be lumped depression storages on the subbasin's surface. The other approach is to represent the SMRs as “reservoirs”, which is the spatially explicit approach.

The change in reservoir storage can be represented as:

$$\frac{dR}{dt} = Q_{in}(t) - Q_{out}(t) \quad (1)$$

Rearranging equation (1)

$$Q_{out}(t) = Q_{in}(t) - \frac{dR}{dt} \quad (2)$$

The inflow into a reservoir from a subbasin is presented in equation (3).

$$Q_{in}(t) = P(t) - ET(t) - \frac{dS(t)}{dt} - \alpha \frac{dD(t)}{dt} \quad (3)$$

Substituting (3) in (2)

$$Q_{out}(t) = P(t) - ET(t) - \frac{dS(t)}{dt} - \alpha \frac{dD(t)}{dt} - \frac{dR}{dt} \quad (4)$$

$$Q_{out}(t) = P(t) - ET(t) - \frac{dS(t)}{dt} - \alpha \frac{dD(t)}{dt} - \beta \frac{dR}{dt} \quad \alpha, \beta \in \{0,1\} \quad (5)$$

where,

Q_{out} is the outflow from the subbasin

P is the rainfall over the subbasin

ET is the evapotranspiration over the subbasin

$\frac{dS(t)}{dt}$ is the change in soil moisture storage over the subbasin

$\frac{dD(t)}{dt}$ is the change in lumped depression storage over the subbasin

$\frac{dR}{dt}$ is the change in reservoir storage

Equation (5) represents the full form of the outflow from the reservoir, where the values of α and β are binary in nature, i.e., they can take the value of either 0 or 1.

To analyze the model structure uncertainty associated with the representation of SMRs in HEC-HMS, four configurations were formulated. Initially, all the SMRs within the subbasin were demarcated. Further, the demarcated SMRs were classified as cascade SMRs (CAS) and catchment outlet SMRs (COS). The medium reservoirs (storage between 1 and 100 Mm^3) at the outlet of the catchments were classified as catchment outlet SMRs (COS), while the other reservoirs, which drained to the COS, were considered as cascade SMRs (CAS).

Four different model structures or model configurations were formulated based on the representation of SMRs within HEC-HMS. Depending on the values of α and β in equation 5, the configuration representations were formulated as presented in Figure 2.

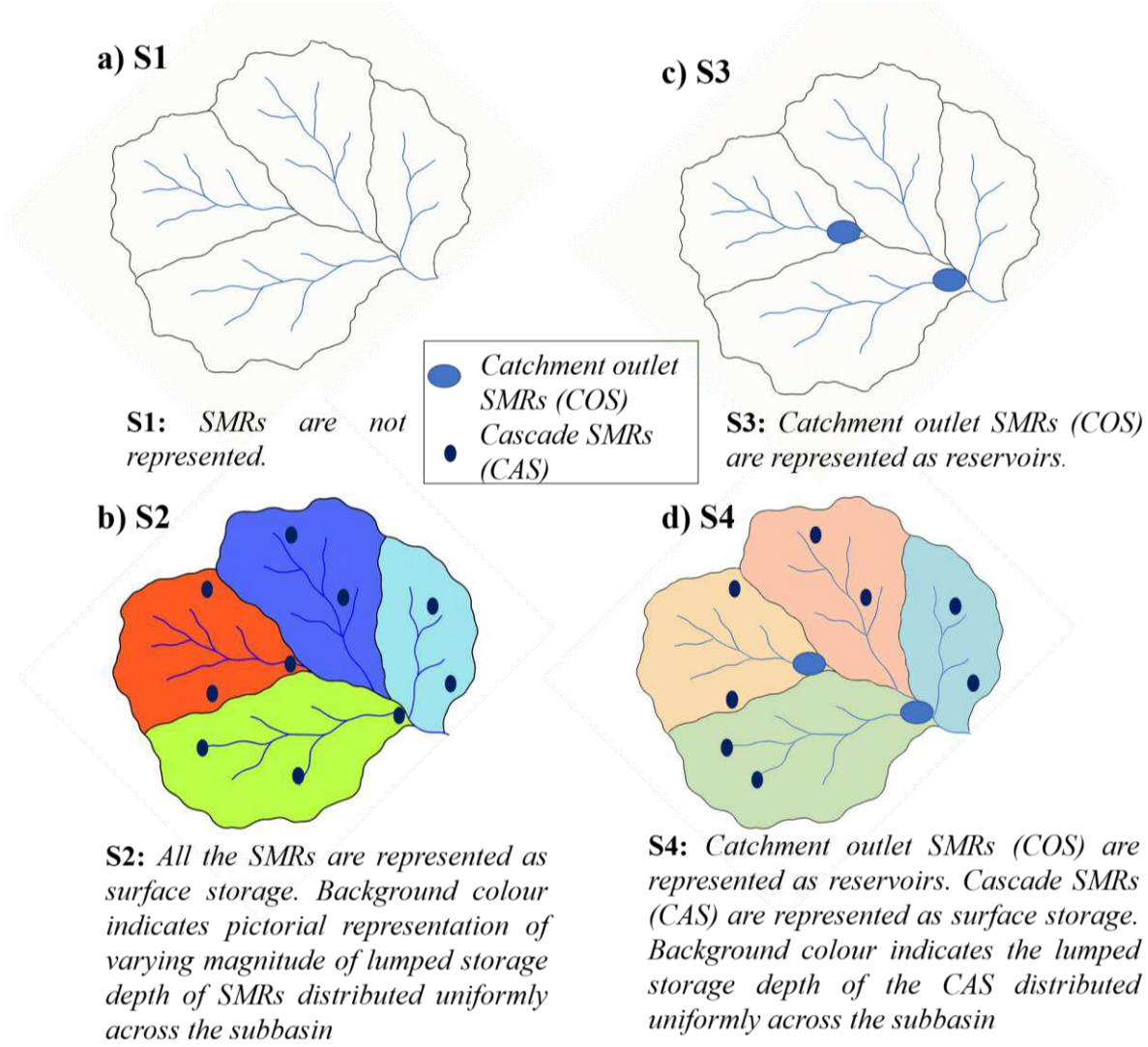


Figure 2. Conceptual representation of the four different model configurations

2.3.1 Configuration 1 (S1) – Modeling without SMRs

In the first configuration, none of the demarcated SMRs were modeled in HEC-HMS. The hydrologic model performance of this configuration will help to compare any improvement in model performance, if any, when the SMRs are represented in the hydrological models. There

are no SMRs in the conceptual representation of S1 as presented in Figure 2a. Substituting the values of $\alpha = 0$ and $\beta = 0$, equation (5) reduces to

$$Q_{out}(t) = P(t) - ET(t) - \frac{dS(t)}{dt} \quad (6)$$

2.3.2 Configuration 2 (S2) – Modeling of all SMRs as lumped surface storages

In the second configuration, both the cascade SMRs (CAS) and catchment outlet SMRs (COS) were modeled as lumped storages within the subbasin, i.e., all the SMRs are represented as "surface storage" (lumped depression storage). The total storage capacity of all the SMRs within the subbasin was divided by the subbasin area, and the resulting value would represent the "depth of depression storage" uniformly distributed across the subbasin. All the SMRs within individual subbasins are combined, and the depth of depression storage is represented as different colors in the conceptual representation of S2 (Figure 2b). Substituting the values of $\alpha = 1$ and $\beta = 0$, equation (5) reduces to:

$$Q_{out}(t) = P(t) - ET(t) - \frac{dS(t)}{dt} - \frac{dD(t)}{dt} \quad (7)$$

2.3.3 Configuration 3 (S3) – Modeling of catchment outlet SMRs (COS) alone as reservoirs

It would be intuitive to consider some of the SMRs (typically SMRs at critical junctions of major water courses) as "reservoirs", rather than considering all SMRs as "surface storage". Therefore, in Configuration 3, only the catchment outlet SMRs (COS) were modeled as "reservoirs", while the CAS draining into the COS were ignored in the modeling exercise. The COS was represented in the hydrological model as "reservoirs". The corresponding Elevation-Storage (E-S) relationship was extracted from the Elevation-Area-Capacity (EAC) relationship available for the SMR from a physical ground survey. From the discharge values computed for each storage level, the Storage-Discharge (S-D) relationship was given as an input for each of the COS in the hydrological model. Configuration 3 has been formulated with the

understanding that data (EAC and S-D) may not be available for all SMRs to be modeled as "reservoirs". For S3, only the COS are represented as "reservoirs" at the subbasin outlet. This is conceptually presented in Figure 2c. Substituting the values of $\alpha = 0$ and $\beta = 1$, equation (5) reduces to:

$$Q_{out}(t) = P(t) - ET(t) - \frac{dS(t)}{dt} - \frac{dR}{dt} \quad (8)$$

2.3.4 Configuration 4 (S4) – Modeling of cascade SMRs (CAS) as lumped surface storages and catchment outlet SMRs (COS) as reservoirs

Although the representation of SMRs as "reservoirs" in HEC-HMS would be most appropriate to model the storage and lag within the subbasin, it would involve data collection on the numerous SMRs within the subbasin. In addition, it would increase the model complexity. In order to overcome this, the S4 configuration was conceptualized using the logical approach of combining the lumped representation in S2 and the spatially explicit representation in S3. As a result, the CAS was represented as lumped "surface storages" distributed uniformly across the subbasin, and COS was represented explicitly as "reservoirs" in the hydrologic model. This representation overcomes the limitation of not representing the CAS in S3 while at the same time requiring minimal data (only storage of the SMRs) to model CAS as "surface storage' as in S2. The depression storage depth of CAS is presented by different colors and the COS is represented as "reservoirs" as conceptually presented in Figure 2d for S4. Substituting the values of $\alpha = 1$ and $\beta = 1$, in equation (5), the equation in its complete form is represented as follows:

$$Q_{out}(t) = P(t) - ET(t) - \frac{dS(t)}{dt} - \frac{dD(t)}{dt} - \frac{dR}{dt} \quad (9)$$

2.4 Parameterization of the SMA loss model and model setup in HEC-HMS

The loss model used was the Soil Moisture Accounting (SMA) model that was parameterized based on the landuse/landcover (LULC), DEM, and soil data. To facilitate the inter-comparison between the model configurations– S1, S2, S3, and S4, the same parameterization was adopted for all four model configurations. The methodology described by Holberg (2014) was adopted for the estimation of SMA parameters such as soil storage capacity ($SoilStore$), soil tension capacity ($SoilTens$), maximum infiltration rate ($MaxSoilInfil$), maximum percolation rate, percentage impervious, and lag time (T_L). All the soil parameters were calculated for each soil class within the subbasin. The area-weighted average value across the subbasin was given as an input to each subbasin in the HEC-HMS model.

From the LULC map available, the impervious area was extracted. The extracted impervious area was overlaid on the delineated subbasins, and the percentage of impervious area in each subbasin was computed.

The transform method used in HEC-HMS was the Soil Conservation Service -Unit Hydrograph (SCS-UH) method. The equations are presented as follows:

$$T_c = \frac{L^{0.8} \times (S+10)^{0.7}}{1140 \times Y^{0.5}} \tag{10}$$

$$T_L = 0.6 \times T_C \tag{11}$$

where,

T_L is the lag time in hours; T_c is the time of concentration in hours; L is the longest flow path in feet; S is the maximum potential retention in mm; Y is the average subbasin slope in %.

The kinematic wave routing method was used for channel routing, and the average monthly evapotranspiration rates were given as inputs to the HEC-HMS model. The same model parameterization was adopted for all the model configurations. However, the model

configuration for SMR representation was done uniquely for each configuration, as discussed previously. The Elevation-Storage (E-S) and Storage-Discharge (S-D) relationship curves were given as an input to the COS. For lumped surface storage, the total storage volume of all the SMRs within a subbasin was combined and divided by the subbasin area to compute the depth of "surface storage". Using the subbasins from the watershed delineation, deduced parameters for each subbasin, and configuration of SMRs, the SMA model was set up in HEC-HMS independently for S1, S2, S3, and S4 model configurations.

2.5 Sensitivity analysis

Sensitivity analysis was carried out to understand the sensitive parameters of the model for the four different model configurations. For this, a reference simulation is required. The reference simulation utilizes the initial parameterized values. The one-at-a-time (OAT) sensitivity analysis was performed. Each of the parameters was independently varied from -50% to +50%, keeping all the other parameters constant. The simulation runs were performed, and the sensitivity of the parameters was compared for two hydrologic variables: the simulated peak inflow and the total inflow volume from the reference simulation. A sensitivity index (I) was computed for each and every parameter in the four different model configurations for the two simulated hydrologic variables. Lenhart et al., (2002) approximated the formula for computing the sensitivity index (I) using the finite difference method as presented in equation (15)

$$I = \frac{(y_{max} - y_{min})/y_{ref}}{(x_{max} - x_{min})/x_{ref}} \quad (12)$$

where, y_{max} and y_{min} refers to the maximum and minimum values of the model outputs (peak inflow and total inflow volume in this case) respectively, x_{max} and x_{min} are the corresponding parameter values at which y_{max} and y_{min} occur respectively, x_{ref} is the average of x_{max} and x_{min} and y_{ref} is the model output corresponding to x_{ref}. A positive sign for I indicates that as

the parameter value increases, the model output value increases, whereas a negative sign indicates a decrease in model output value as the parameter value increases. Irrespective of the sign, a value of I close to 0 signifies small to negligible sensitivity, and a value of I close to 1 signifies high sensitivity. I can have values greater than 1 which signify very high sensitivity.

2.6 Uncertainty analysis

The uncertainty analysis manager in HEC-HMS uses Monte Carlo simulations to address the parameter uncertainty. The simple distribution sampling method is used to define the uncertainty in a particular parameter. The generation of a set of parameters cannot be done within HEC-HMS. However, there is a specified values sampling method which allows the user to specify one or more sequences of parameter values (USACE 2025). Bhavsar and Patel (2020) carried out uncertainty analysis for the initial abstraction, Curve Number (CN), and percentage impervious parameters by generating uniform random parameter sets for conducting 244 model simulations. Assuming uniform distribution is a good choice in the case of the non-availability of existing knowledge on parameters. In this context, the Latin Hypercube Sampling (LHC) offers an advantage in that the variance is less asymptotic than the one obtained from simple random sampling (Stein 1987). LHC improves upon the simple random sampling and is a good method to use for selecting values of input variables (McKay et al. 2000). Hence, in this study, the LHC approach is combined with the HEC-HMS model to quantify the model structural and parameter uncertainties due to the representation of SMRs in HEC-HMS for flood simulations.

The range for the sampling of parameters was given as -30% to + 30% from the parameterized values. Uniform distribution was assumed for the parameters. The 15000 parameter sets generated using the LHC approach were given as input to each of the subbasins in the HEC-

HMS model. The HEC-HMS was simulated externally using '*pyhecdss'* tools available in Python.

2.8 Simulation of S1, S2, S3, and S4 model configurations

Using the generated parameter sets and the independent model setup for the model configurations – S1, S2, S3, and S4, the continuous simulations were done. The initial storage of the catchment outlet SMRs (COS) modelled as "reservoirs" plays a vital role in the simulations. Therefore, the COS in S3 and S4 were simulated with various initial storage levels – 0%, 25%, 50%, and 75% of the maximum storage. The performance metrics were computed and analyzed. The best performing model from S3 and S4, based on the initial condition, was compared with the S1 and S2 model configurations to benchmark the performance of the hydrological model for continuous flood simulations.

2.9 Quantification of model structure uncertainty and parametric uncertainty

To distinguish between model structure and parametric uncertainties associated with the representation of SMRs from an ensemble of outputs, a variance decomposition approach was used (Yip et al. 2011; Ma et al. 2018). The total variance was decomposed as the sum of model variance, parametric variance, and residual variance. The residual variance captures numerical errors, stochastic variability, and any unexplained variation. Each model structure was evaluated with the same number of parameter sets, ensuring a balanced design.

The total variation is considered as given in equation (13)

$$SS_T = SS_M + SS_P + SS_R \tag{13}$$

Each of the terms in equation (13) is computed as follows:

$$\bar{Y} = \frac{1}{mn}\sum_{i=1}^{m}\sum_{j=1}^{n} x_{i,j} \tag{14}$$

$$SS_T = \sum_{i=1}^{m}\sum_{j=1}^{n}(x_{i,j} - \bar{Y})^2 \quad (15)$$

$$[\bar{Y}_l] = \frac{1}{n}\sum_{j=1}^{n} x_j \quad (16)$$

$$SS_M = n\sum_{i=1}^{m}(\bar{Y} - \bar{Y}_l)^2 \quad (17)$$

$$[\bar{Y}_J] = \frac{1}{m}\sum_{i=1}^{m} x_i \quad (18)$$

$$SS_P = m\sum_{j=1}^{n}(\bar{Y} - \bar{Y}_J)^2 \quad (19)$$

where,

SS_T is the total variation in outputs

SS_M is the variation between model configuration or structure

SS_P is the variation between parameters

SS_R is the unexplained variation

$x_{i,j}$ is the inflow of the i^{th} model for the j^{th} parameter set

m and n are the number of model configurations and parameter sets, respectively.

The proportion of model variance, parameter variance, and residual variance was computed using the inflow for each time step and averaged across all time steps. The average contribution of model structure variance and parameter variance to the total variance was computed. Thus, this study differentiates the model structure uncertainty and parametric uncertainty associated with the representation of SMRs in flood simulations.

3. Study Area

Chembarambakkam catchment in the upstream of Adyar subbasin in south India is taken as the case study for this work. The Chembarambakkam catchment has an area of around 380 km^2.

The catchment culminates at the Chembarambakkam reservoir, which is a major source of drinking water for the city of Chennai, with a storage capacity of around 103 Mm^3. The index map of the study area is presented in Figure 3. The upstream of the Chembarambakkam reservoir has a large number of interconnected SMRs. The medium reservoirs (storage between 1 and 100 Mm^3) at the outlet of the catchments were classified as catchment outlet SMRs (COS), while the other reservoirs, which drained to the COS, were considered as cascade SMRs (CAS). The major catchment outlet SMRs (COS) are Nemam (1), Sriperumbudur (2), and Pillaipakkam (3) with a storage capacity of 20.352 Mm^3, 8.514 Mm^3, and 4.35 Mm^3, respectively. In addition to these COS, there are hundreds of SMRs (CAS) that drain into the COS which were considered as CAS. During the active North-East Monsoon period, from November to December, it becomes essential to accurately simulate the inflow to Chembarambakkam for the operation of the reservoir. Hence, the Chembarambakkam catchment is selected as the study area.

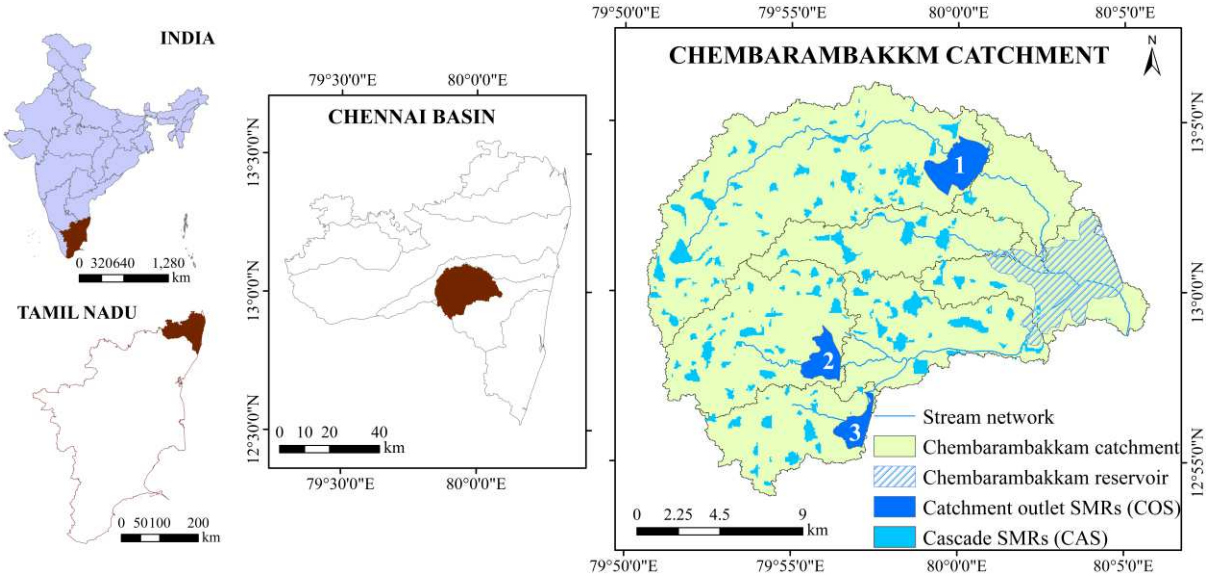


Figure 3. Index map of the study area

3.1 Datasets used for the study

The Digital Elevation Model (DEM) used in the study was the Shuttle Radar Topography Mission (SRTM). SRTM DEM was improved based on the burn-in streams obtained using a high-resolution hydrographic survey. The COS were also considered during the watershed delineation process so that the model represents the physical processes as closely as possible. With the improved DEM and the location of the COS, the subbasins were delineated.

The DEM used for the Chembarambakkam catchment was the improved SRTM with stream burnt into it at 30m spatial resolution. The Tamil Nadu Agricultural University (TNAU) soil data at a 1:50000 scale was used for the soil parameterization. The parameterized values for each subbasin according to the SMA model are presented in Figure 4.

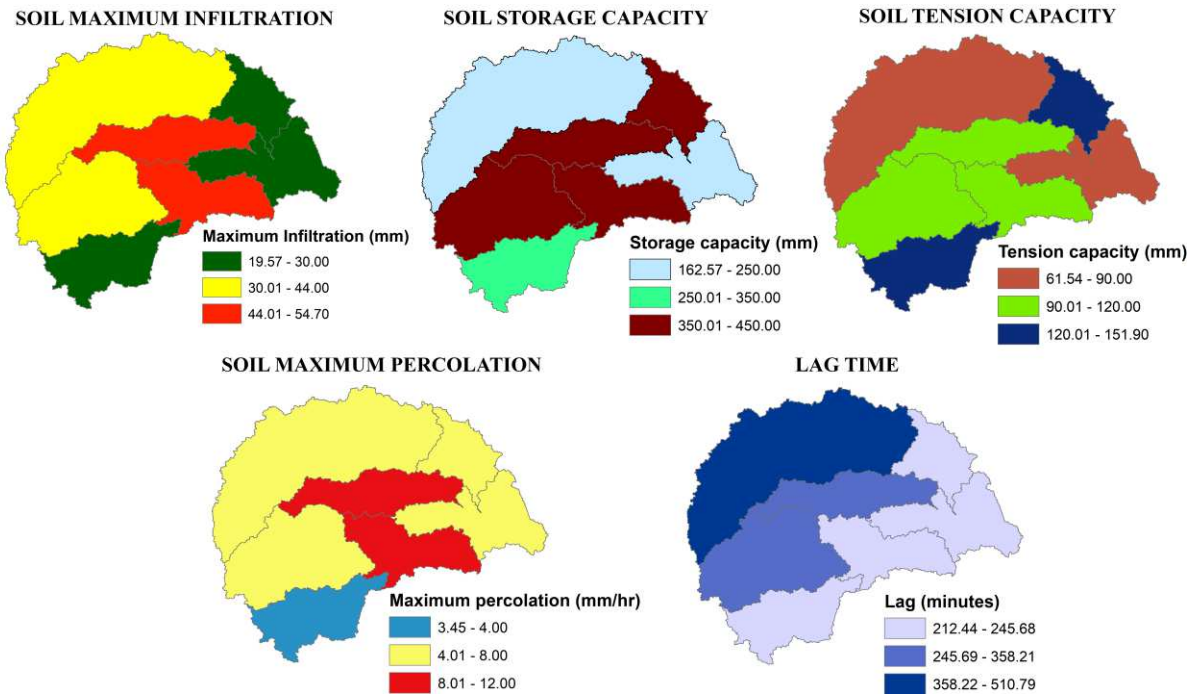


Figure 4. Spatial variation of the HEC-HMS model parameters

The land-use/land-cover (LULC) data, obtained from the National Remote Sensing Center (NRSC) for the year 2019, were used at a 56m spatial resolution. To represent the spatial variation of rainfall in the hydrological model, the Thiessen polygon method was considered to convert the point rainfall data to areal precipitation for each subbasin in the HEC-HMS

model. The hourly observed rainfall data from rain gauge stations were used to account for the spatial and temporal variation in rainfall. For the calibration and validation of the hydrological model, the observed inflow values to the Chembarambakkam reservoir were obtained from the Water Resources Department (WRD), Government of Tamil Nadu (GoTN), at an hourly scale during the times of heavy inflow.

Four different model structures were considered as configurations- S1, S2, S3, and S4. S1 does not incorporate any of the SMRs into its model configuration. S2 represents both the CAS and COS as lumped "surface storages" in the HEC-HMS model. As not all the SMRs can be represented as "reservoirs", S3 represents the COS alone as "reservoirs" in its model configuration in HEC-HMS. S4 was conceptualized as a combination of configurations S2 and S3. In the S4 model configuration, the CAS were represented as lumped "surface storages" and the COS as "reservoirs" in the HEC-HMS model. The model structure in HEC-HMS for the four configurations is presented in Figure 5. The data for the SMRs was collected from the Water Resources Department (WRD), Government of Tamil Nadu (GoTN). The hydraulic particulars and bathymetry data were available for the COS. It was used in the parameterization of Storage-Discharge (S-D) relationship for the COS in S3 and S4 configurations. However, only the total storage capacity data was available for the CAS which was used in the parametrization of "surface storages" as explained in Section 2.3.2. The HEC-HMS model was set up independently for all four configurations, and the simulations were carried out. Table 1 presents the storage capacity of SMRs modeled as "surface storages" and as "reservoirs" in each of the four configurations.

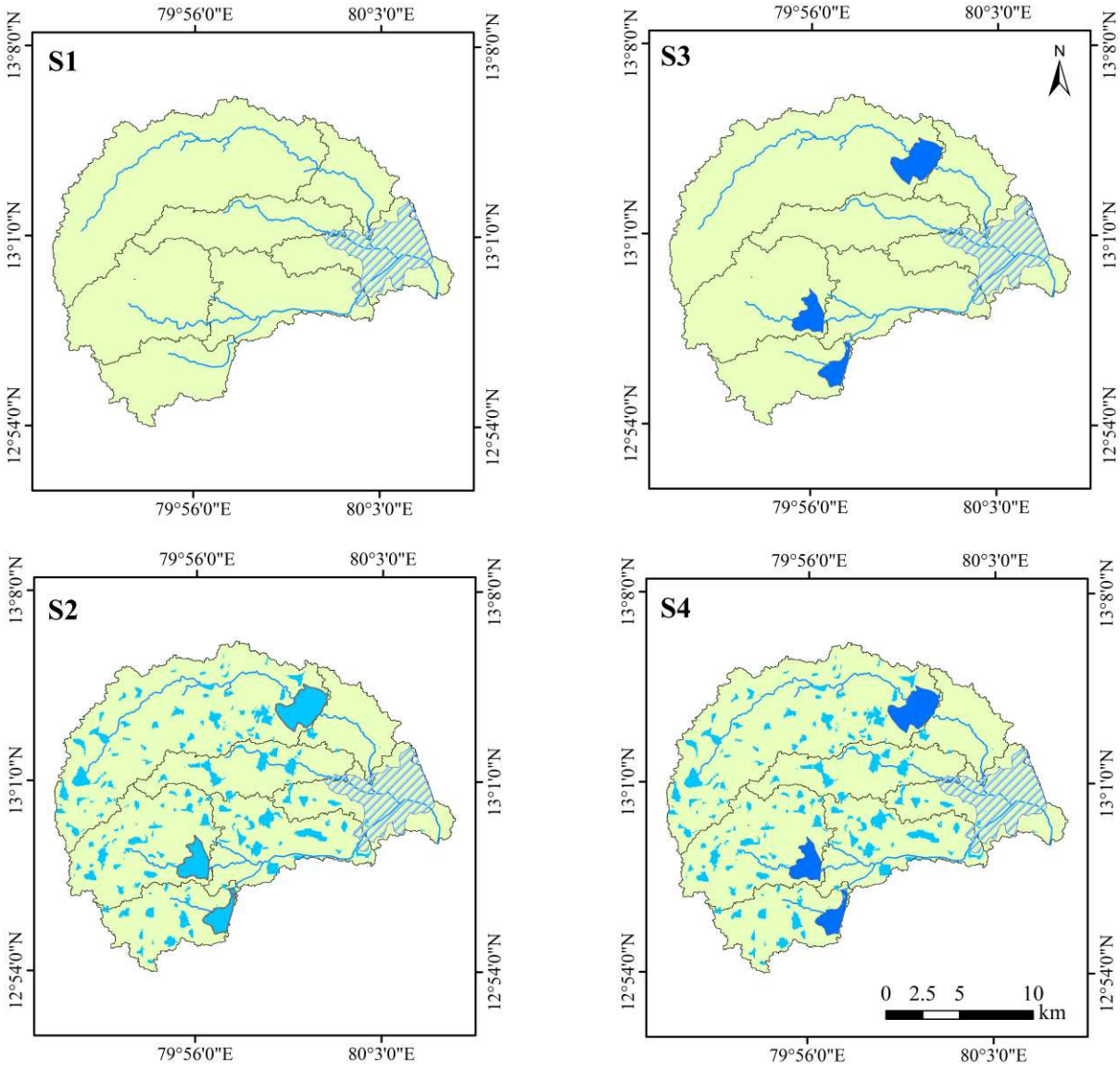


Figure 5. Model configuration of the four different configurations

Table 1. Storage (Mm^3) incorporated in the various configurations

Configuration	Surface Storage (Mm^3)	Reservoir (Mm^3)
S1	0	0
S2	59.484	0
S3	0	33.217
S4	26.267	33.217

Even during the North East Monsoon period, the flow is highly skewed to a few days in the months of November. However, during the North-East Monsoon (NEM) of 2021, the number of days with significant flow was relatively high. The major synoptic-scale systems in November 2021 included a low-pressure area as well as a depression over the Bay of Bengal (BoB). The month started with the 01st to 04th of November receiving rainfall because of the low-pressure area over the BoB, followed by two depressions (10th and 11th of November 2021 & 18th and 19th of November 2021). In addition, the rainfall was distributed evenly throughout the entire month of November 2021, rather than confined to a few specific days, and has therefore been selected for the study. Hence, NEM 2021 was taken for the sensitivity analysis and calibration of the hydrological model. The model structure uncertainty and parameter uncertainty associated with the representation of SMRs were quantified. The NEM 2023 was used for the validation of the hydrological model. The performance of the hydrological model for the four configurations, during both calibration and validation, was analyzed.

3.2 Hydrologic model performance assessment

The Nash Sutcliffe Efficiency (NSE) was computed for each simulation, and the simulations that had an NSE value greater than 0.4 were considered as behavioral solutions. In this manner, the HEC-HMS simulations were done for each of the four configurations. Using the observed flow data, the performance metrics were computed.

Nash Sutcliffe Efficiency (NSE) is computed as the ratio of the error variance of the modeled discharge to the variance of the observed discharge. NSE value ranges from -∞ to +1. NSE measures relative error with respect to the observed mean. A high value of NSE, i.e., close to 1, means good model performance, whereas negative values of NSE indicate that the mean of the observed values is a better estimate than the model.

$$NSE = 1 - \frac{\sum_{t=1}^{T}(Q_m^t - Q_o^t)^2}{\sum_{t=1}^{T}(Q_o^t - \overline{Q_o})^2} \quad (15)$$

The coefficient of determination (R^2) measures the proportion of variance explained by the model when compared with observed values. R^2 generally ranges from 0 to 1. A value of 0 refers to poor model performance, and a value of 1 refers to good model performance.

$$R^2 = \left(\frac{\sum_{t=1}^{T}(Q_m^t - \overline{Q_m})(Q_o^t - \overline{Q_o})}{\sqrt{\sum_{t=1}^{T}(Q_m^t - \overline{Q_m})^2}\sqrt{\sum_{t=1}^{T}(Q_o^t - \overline{Q_o})^2}}\right)^2 \quad (16)$$

Root Mean Square Error (RMSE) refers to the average squared difference between observed and modeled values. RMSE measures absolute error and accounts for both bias and variance. RMSE is always positive, and a value close to zero denotes a good match between observed and simulated values.

$$RMSE = \sqrt{\frac{1}{n}(Q_o^t - Q_m^t)^2} \quad (17)$$

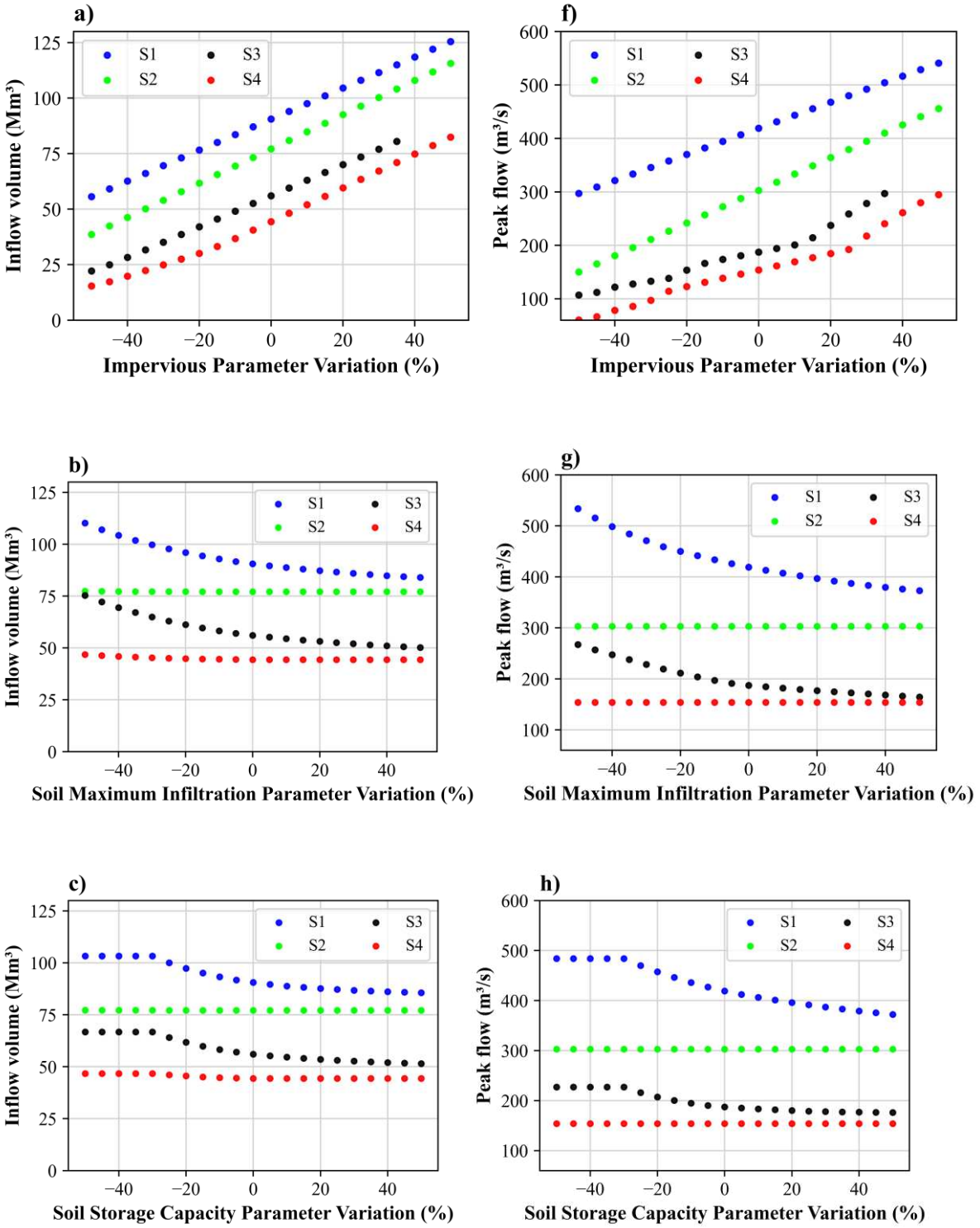
To analyze the model's performance based on the ensemble of hydrographs from the behavioral simulations, an NSE threshold of 0.4 was chosen, and the p-factor was computed. P-factor is the percentage of observed data points enveloped by the ensemble hydrograph. It is computed as the ratio of the number of points within the envelope to the total number of points considered. For the calibration of the hydrological model, NSE was considered as the metric. Based on the maximum NSE value, the calibrated model parameter values were extracted, which were used for the validation of the model. Thus, the developed methodology was applied to quantify the uncertainties associated with the representation of SMRs.

4. Results

4.1 Sensitivity analysis

The model configurations - S1, S2, S3, and S4 were set up, and the sensitivity analysis was carried out for the parameters, namely imperviousness, lag, soil maximum infiltration, soil

storage capacity, and soil tension capacity. The results of the sensitivity analysis are presented in Figure 6 a) to j).



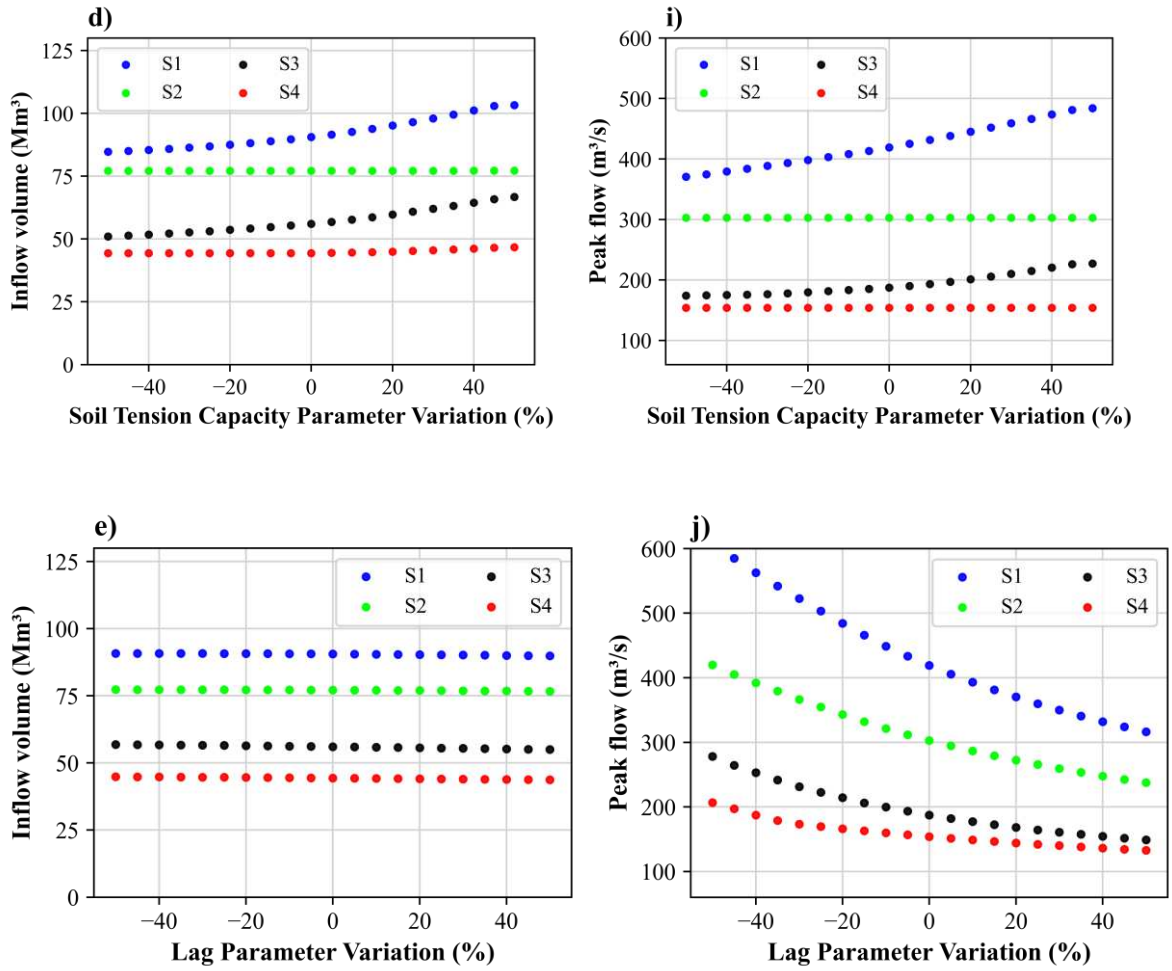


Figure 6. Variation in inflow volume and peak flow for the four different configurations for parameter variation (%)

As expected, the peak inflow and the total inflow volume increase with an increase in the imperviousness parameter for all four model configurations – S1, S2, S3, and S4. The imperviousness parameter had the highest sensitivity index *I* value for S2 (1.009), S3 (1.071), and S4 (1.522) for peak inflow. On the contrary, for the S1 configuration, the lag parameter (-0.696) had the highest sensitivity for peak inflow. All four configurations showed the highest sensitivity of inflow volume to the impervious parameter. At the same time, the lag parameter was not sensitive to inflow volume (*I* value was close to zero). In contrast, a non-linear relationship with a decreasing tendency (negative I value) was observed in the sensitivity of peak inflow to the lag parameter across all four configurations.

For the S2 and S4 configurations, both the inflow volume and peak inflow were not sensitive to parameters such as soil maximum infiltration, soil storage capacity, and soil tension capacity (*I* value close to zero). On the contrary, for S1 and S3 configurations, a non-linear relationship was observed in the sensitivity of inflow volume and peak inflow to the soil parameters (*I* values ranging from -0.4 to -0.2). This behavior is observed because S2 and S4 have a lumped representation of SMRs, which appears to dominate the influence of soil parameters. Meanwhile, in S1 and S3, the absence of a lumped representation of SMRs results in both inflow volume and peak inflow being sensitive to soil parameters. Therefore, the different representation of SMRs in the four configurations considered resulted in different sets of sensitive parameters, leading to varied watershed responses. This sensitivity analysis demonstrates the importance of distinguishing between model structural uncertainty and parametric uncertainty associated with the representations of SMRs for flood simulations.

4.2 Performance assessment of continuous simulations

4.2.1 Performance evaluation of S3 and S4 under varying initial conditions

In configurations S3 and S4, the catchment outlet SMRs (COS) are represented as “reservoirs”. The initial condition of the reservoir plays a significant role in the simulations. However, the initial storage for many of these SMRs is not actively monitored. Hence, it is necessary to assess the uncertainty associated with the reservoir's initial condition to evaluate hydrologic model performance for configurations S3 and S4. To assess uncertainty due to initial conditions, the initial storage in the reservoir was set to 0% (S3a), 25% (S3b), 50% (S3c), and 75% (S3d). The same set of initial conditions was used for S4: S4a (0%), S4b (25%), S4c (50%), and S4d (75%). The hydrological model was simulated for all the LHC parameter sets across the various initial conditions of S3 and S4.sThe violin plots of NSE, R^2, and RMSE for

different initial conditions in the S3 and S4 configurations are shown in Figures 10 and 11, respectively.

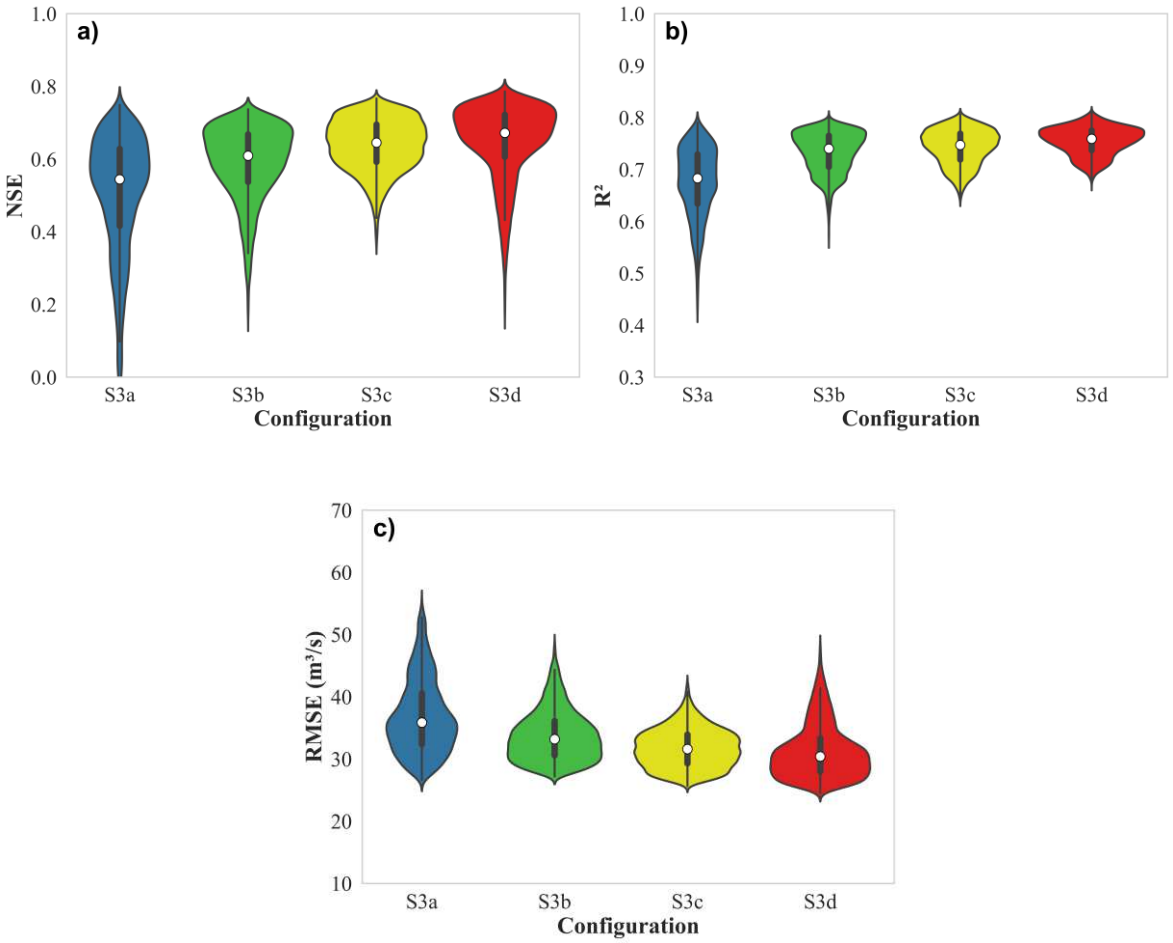
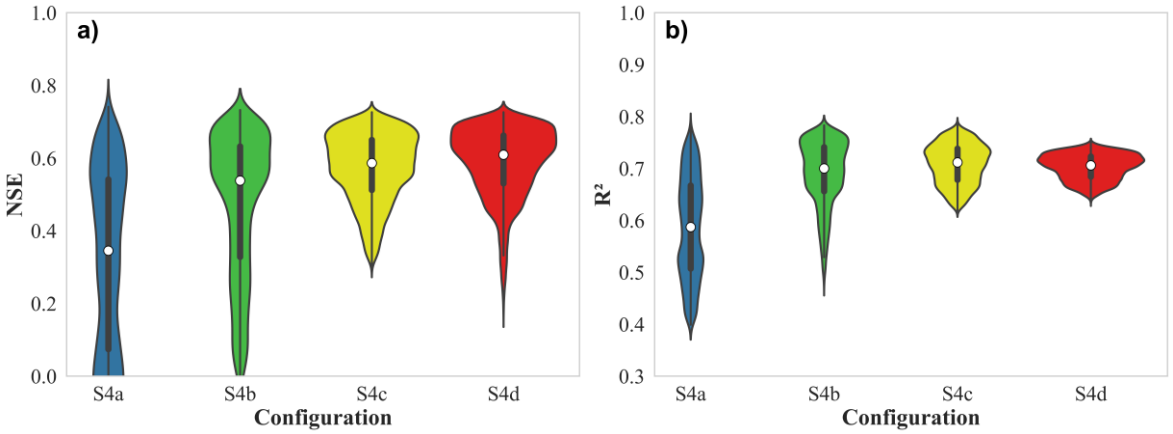


Figure 7. Violin plots of performance metrics for the S3 configuration under different initial conditions



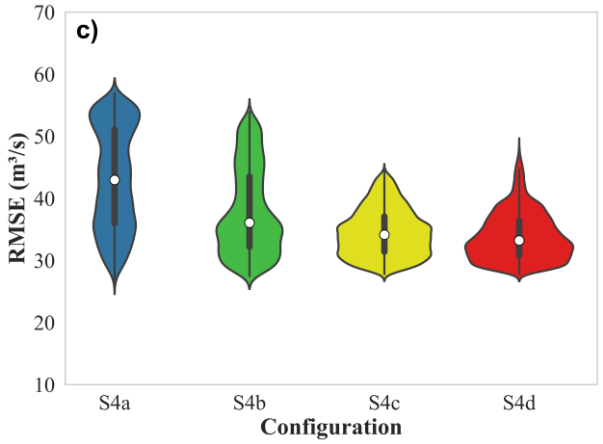


Figure 8. Violin plots of performance metrics for the S4 configuration under different initial conditions.

For the S3 configuration, Figure 7 shows that many simulations have higher NSE and R^2 and lower RMSE for S3d (75% initial storage). A similar pattern was observed for the S4 configuration (Figure 8), where S4d (75% initial storage) also demonstrated enhanced performance. Based on the numerical values, the maximum NSE for S3 and S4 was observed for S3d and S4d, respectively, at 0.786 and 0.726. The median NSE was also higher for S3d (0.672) and S4d (0.609) among their respective configurations. The maximum R^2 among the S3 configurations was for S3d (0.812), and among the S4 configurations was for S4c (0.786). The median RMSE was minimum for S3d (30.4 m^3/s) and S4d (33.212 m^3/s). This again suggests that the COS within the model domain were at a storage level of 75% prior to the start of the continuous simulation analyzed in this study.

4.3.2 Performance evaluation of the model configurations for the continuous simulations

For the performance assessment of the continuous simulations, the S1 and S2 configurations were compared with the best-performing configurations from S3 and S4, i.e., S3d and S4d, respectively. The results are presented as violin plots in Figure 9.

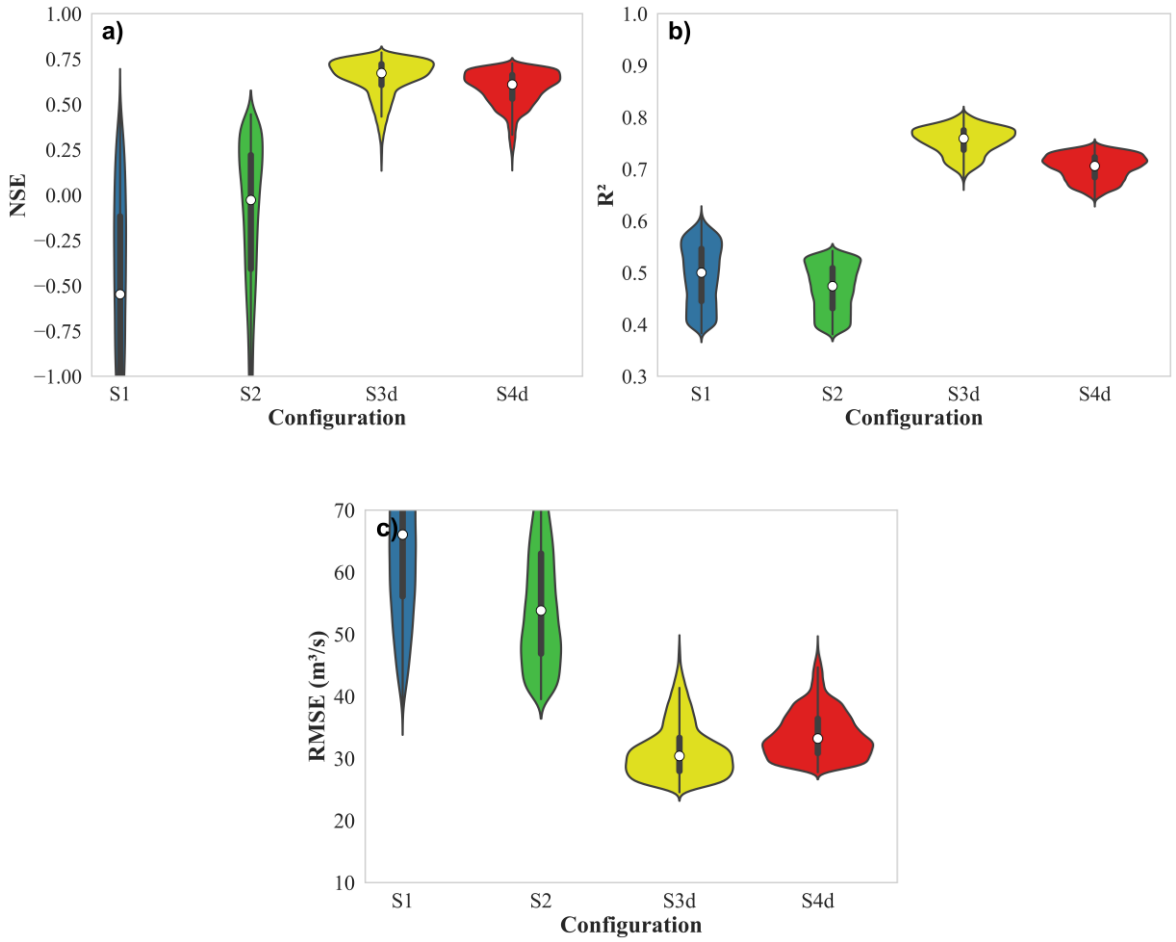


Figure 9. Violin plots of the performance metrics for continuous simulations of the various configurations

The maximum NSE was observed to be less than 0.5 for S1 (0.488) and S2 (0.445), whereas it was greater than 0.7 for S3d (0.786) and S4d (0.726). In addition to the maximum NSE, the median NSE also improved from -0.548 for S1 to 0.672 and 0.609 for S3d and S4d, respectively, due to the realistic representation of SMRs in the models. The maximum R^2 for S1 and S2 was 0.611 and 0.542, respectively, while the minimum R^2 for S3d and S4d itself was 0.668 and 0.635, respectively. The violin plots of R^2 show a distinct separation, with S3d and S4d exhibiting higher values than S1 and S2. The median RMSE also indicated that S3d (30.4 m^3/s) and S4d (33.21 m^3/s) showed improved performance over S1 (66.05 m^3/s) and S2 (53.82

m^3/s). In addition, the RMSE was also comparatively higher for S1 and S2 (in the range of 37 m^3/s to 112 m^3/s for S1 and 39 m^3/s to 87 m^3/s for S2), whereas it was only in the range of 24 m^3/s to 49 m^3/s for S3d and S4d. This reveals that both the range and median of RMSE were lower for S3d and S4d than for S1 and S2. In addition to the above results, the incorporation of COS as "reservoirs" in the model configurations of S3 and S4 (irrespective of the initial condition) improved hydrologic model performance compared to S1 and S2. Again, this indicates the importance of appropriately representing SMRs in realistically simulating the hydrologic response for flood simulations.

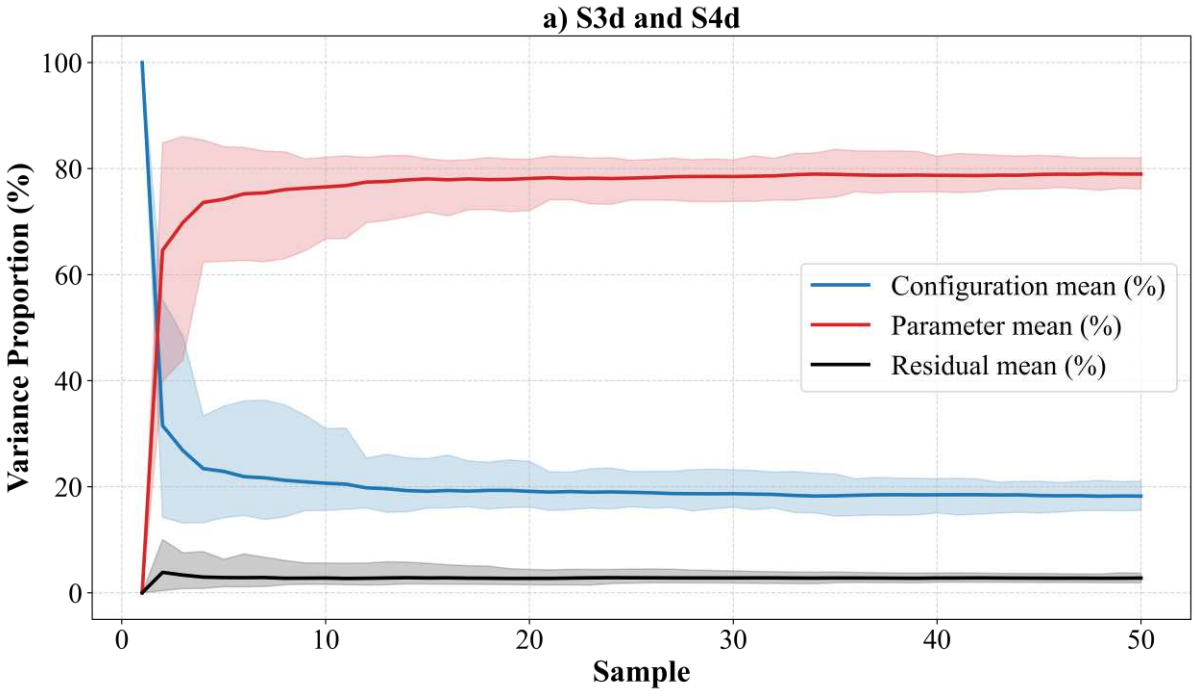
4.4 Quantification of model structure uncertainty and parametric uncertainty

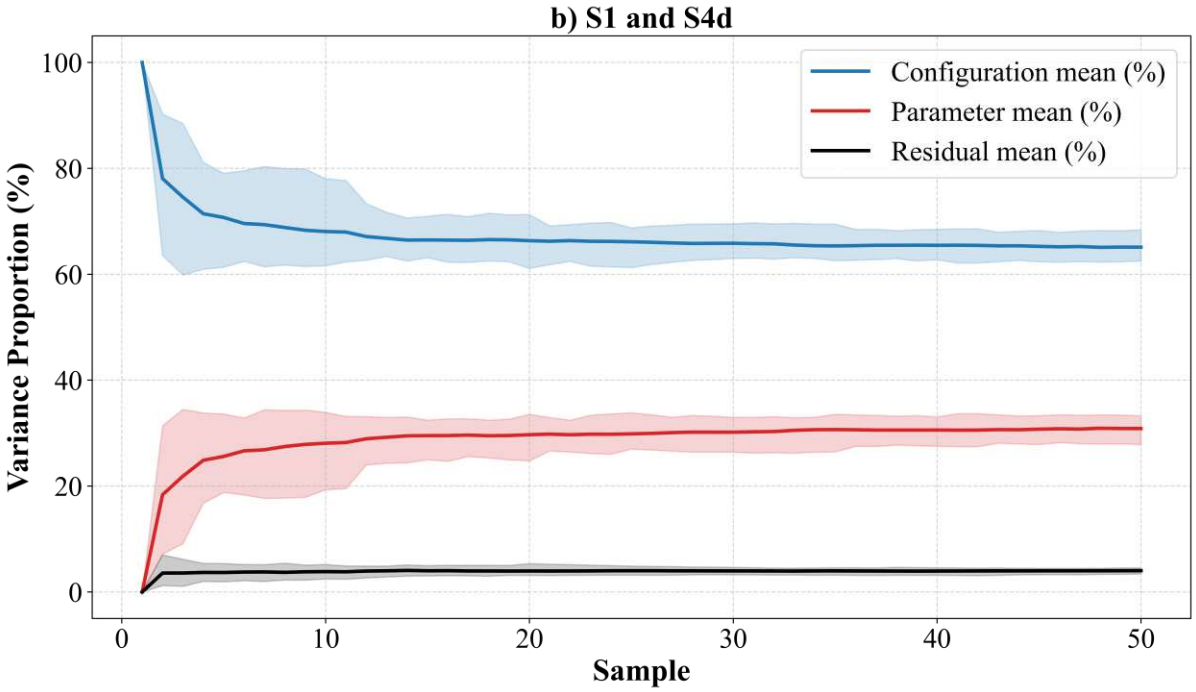
The improvement in model performance of S3 and S4 configurations (with explicit representation of SMRs in the model) compared to S1 and S2 configurations (without explicit representation of SMRs in the model) was demonstrated in the previous section. To distinguish model structure uncertainty from parameter uncertainty in the continuous simulation, a variance decomposition analysis combined with a bootstrapping procedure was conducted, using the time series of inflow values.

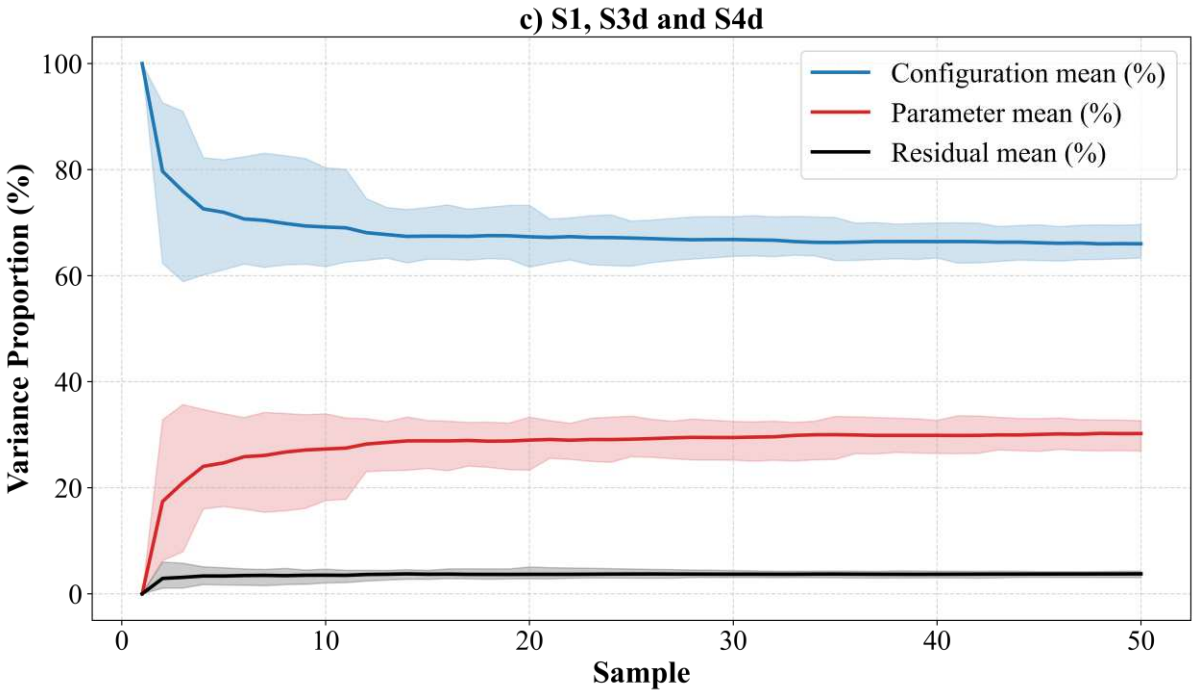
From the simulations carried out, the simulations with NSE > 0 were filtered out and used to quantify the uncertainties. The total variance, model variance, and parameter variance were found from a randomly selected sample of 50 simulations. The convergence of the computation of the variance was tested by repeating the analysis over 20 realizations. The variance decomposition was done for each time step of the inflow value and averaged across the time steps. The analysis was conducted for all pairwise combinations (S1–S2, S1–S3d, S1–S4d, S2–S3d, S2–S4d, and S3d–S4d), all three-configuration combinations (S1–S2–S3d, S1–S2–S4d, S1–S3d–S4d, and S2–S3d–S4d), and the combination including all configurations (S1–S2–S3d–S4d). This analysis will enable an understanding of the uncertainty associated with the

different representations of SMRs for flood simulations. The convergence results for representative configurations are presented in Figure 9.

For S1 and S2, the proportion of parameter variance $(88.46 \pm 3.33\%)$ dominated over the proportion of model variance $(9.91 \pm 2.73\%)$. The major difference between the model structure of S1 and S2 is the inclusion of SMRs as "surface storages" (lumped depression storage) in S2. This is also the model structure difference between S3d (only COS) and S4d (COS as reservoirs + CAS as surface storage). A similar trend was observed for the analysis of S3d and S4d with varying magnitude values as presented in Figure 9a. Therefore, including SMRs as lumped depression storage led to parametric uncertainty being predominant than model structure uncertainty.




b) S1 and S4d
Configuration mean (%)
Parameter mean (%)
Residual mean (%)
Variance Proportion (%)
Sample
0
20
40
60
80
100
0
10
20
30
40
50


c) S1, S3d and S4d
Configuration mean (%)
Parameter mean (%)
Residual mean (%)
Variance Proportion (%)
Sample
0
20
40
60
80
100
0
10
20
30
40
50

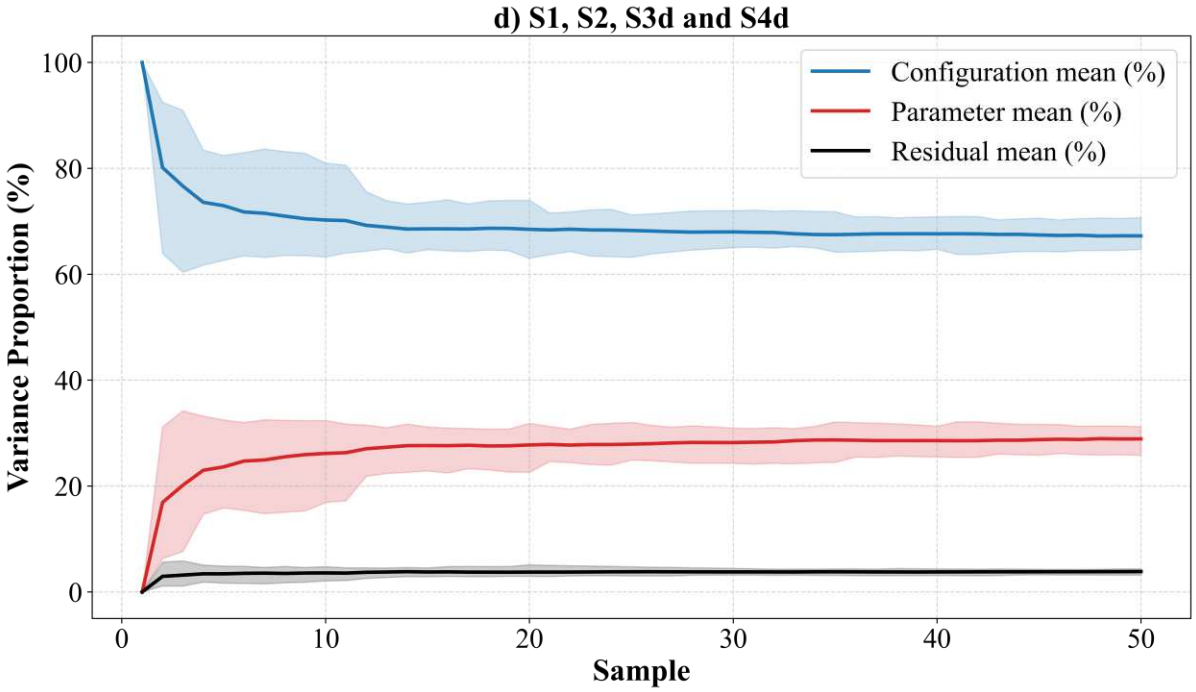


Figure 9. Convergence of the variance proportions for a) S3d and S4d b) S1 and S4d c) S1, S3, S4d and d) S1, S2, S3d, S4d

However, the inclusion of COS as "reservoirs" increased the model structure uncertainty. For the combination of S1 and S3d, the proportion of model variance was $64.58 \pm 4.803\%$, whereas the proportion of parameter variance was $32.26 \pm 4.19\%$. Similar observations with varying magnitude could be made from the results of S1 and S4d as presented in Figure 9b.

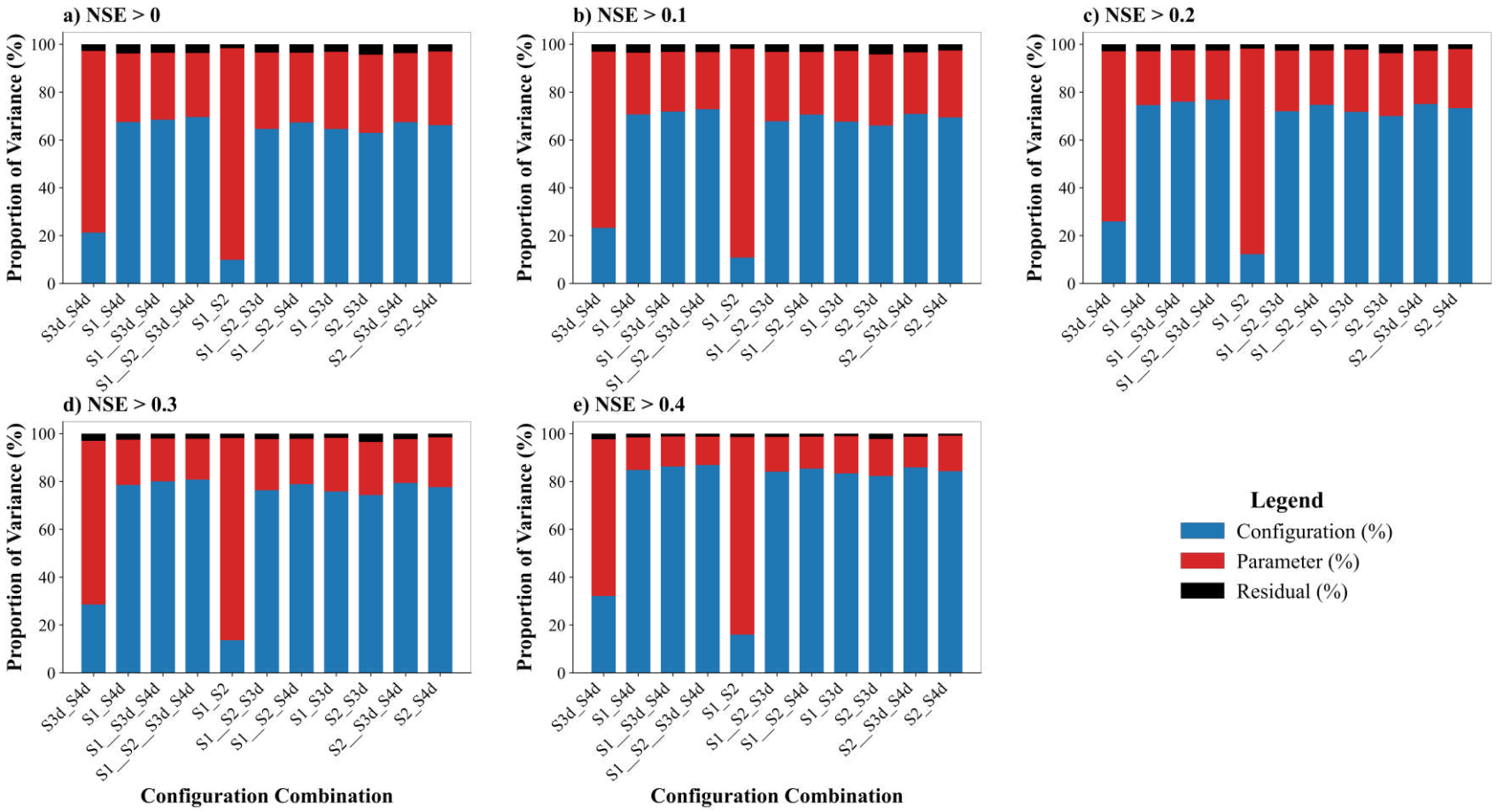


Figure 10. Variance proportion analysis across configuration combinations for a) NSE > 0 b) NSE > 0.1 c) NSE > 0.2 d) NSE > 0.3 e) NSE>0.4

The results when all four configurations, S1, S2, S3d, and S4d, were included in the analysis are presented in Figure 9d. The proportion of model variance to total variance was found to converge at $69.58 \pm 5.08\%$. The proportion of parametric variance and residual variance was at $26.76 \pm 4.54\%$ and $3.66 \pm 0.90\%$ respectively.

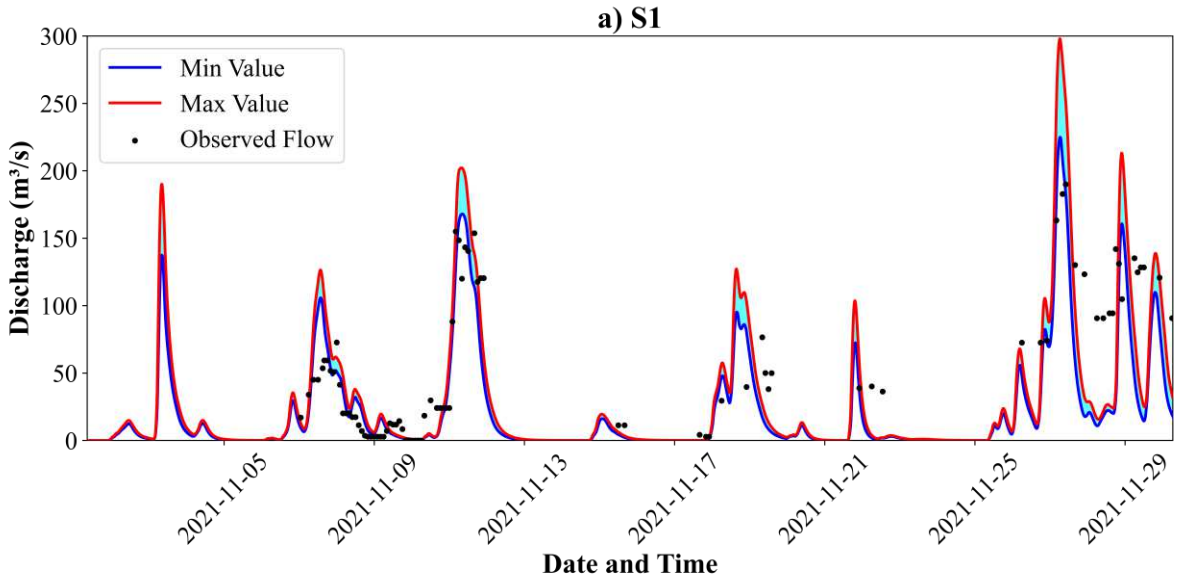
The proportion of model, parameter, and residual variance for all combinations of configurations for increasing values of NSE is reported in the form of a stacked column in Figure 10. Irrespective of the NSE value, out of the 11 configurations analyzed, 9 configurations resulted in model structure uncertainty dominating the parameter uncertainty. Only for the two combinations of S1 & S2 and S3d & S4d, the parametric uncertainty dominates the model structure uncertainty. However, for all combinations, the proportion of model structure uncertainty increased as the NSE value increased from 0 to 0.4. For the NSE > 0.4 case, when S1, S2, S3d, and S4d were considered, the proportion of model variance to total variance was found to converge at $86.86 \pm 2.37\%$ which is very high compared to the proportion of parametric variance of $11.88 \pm 2.27\%$. The proportion of residual variance was $1.26 \pm 0.28\%$. Thus, it can be concluded that in the representation of SMRs, the model structure plays a significant role, and model structure uncertainty is dominant over parametric uncertainty. Therefore, the representation of SMRs needs to be done appropriately and strategically in hydrological models for accurate flood simulations.

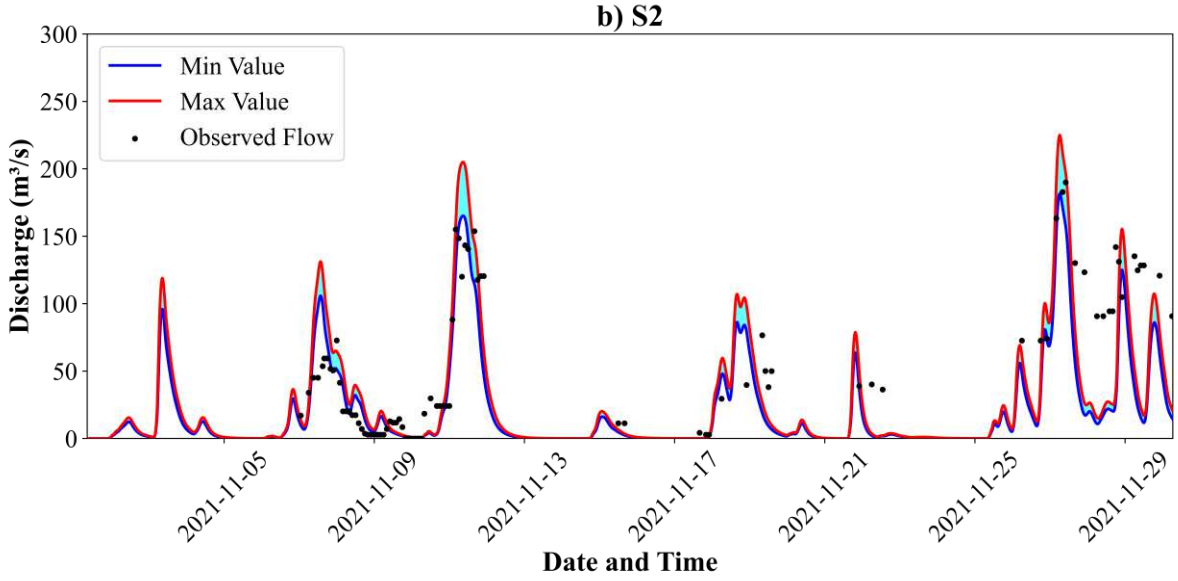
4.4 Calibration of the hydrological model

For calibration of the hydrological model, NSE was used as the objective function. Simulations that exceeded the NSE threshold of 0.4 were selected as behavioral solutions. For every time step across the entire simulation duration, the minimum and maximum values of the hydrograph from the behavioral solutions were computed for each of the four configurations. Thus, the spread of behavioral hydrographs was plotted, and the p-factor was computed. The

results showed that there was an increase in the p-factor value from 0.078 for S1 to 0.449 for S3d. However, there was a marginal increase in the p-factor value from S1(0.078) to S2(0.112). This is mainly because of the smaller number of simulations for S1 (140) and S2 (601) above the threshold NSE > 0.4. The p-factor value for S4d was recorded as 0.415. The spread of the behavioral hydrographs or the uncertainty band of the hydrograph plotted for the condition NSE > 0.4 is presented in Figure 11 for all four configurations.

At the start of the simulation, the upper envelope of the hydrograph is higher for S1 than for all other configurations. This is because SMRs are not represented in these configurations, leading to less watershed storage and increased runoff response. To neutralize the effect of the basin's initial conditions, the initial hydrograph was not included in the computation of the performance metrics. In addition, the upper envelope of the hydrograph is consistently higher for S1 than for the other three configurations. In the S1 and S2 configurations, the lower envelope of the hydrograph is consistently higher than in S3d and S4d. This implies that configurations S1 and S2 exhibit a watershed response inclined toward runoff generation in comparison to S3d and S4d. As a result, some of the peaks of the observed hydrograph fall just outside the envelope area of the hydrograph for S1 and S2. In contrast, in S3d and S4d, the peaks of the hydrograph mostly fall in the center between the upper envelope and lower envelope. The decreased envelope area under the hydrographs for S1 and S2 results in a lower p-value. Due to the representation of COS as “reservoirs” in S3d and S4d configurations, the envelope area captures the recession limb of the hydrograph. This may be due to the observed lag in watershed response, which is absent in S1 and S2 because COS are not represented as “reservoirs”. Thus, it can be seen qualitatively that the representation of COS as “reservoirs” in S3 and S4 can reasonably capture the peaks as well as the recession limb when compared to S1 and S2.


a) S1
Min Value
Max Value
Observed Flow
Discharge (m³/s)
300
250
200
150
100
50
0
2021-11-05
2021-11-09
2021-11-13
2021-11-17
2021-11-21
2021-11-25
2021-11-29
Date and Time


b) S2
Min Value
Max Value
Observed Flow
Discharge (m³/s)
300
250
200
150
100
50
0
2021-11-05
2021-11-09
2021-11-13
2021-11-17
2021-11-21
2021-11-25
2021-11-29
Date and Time

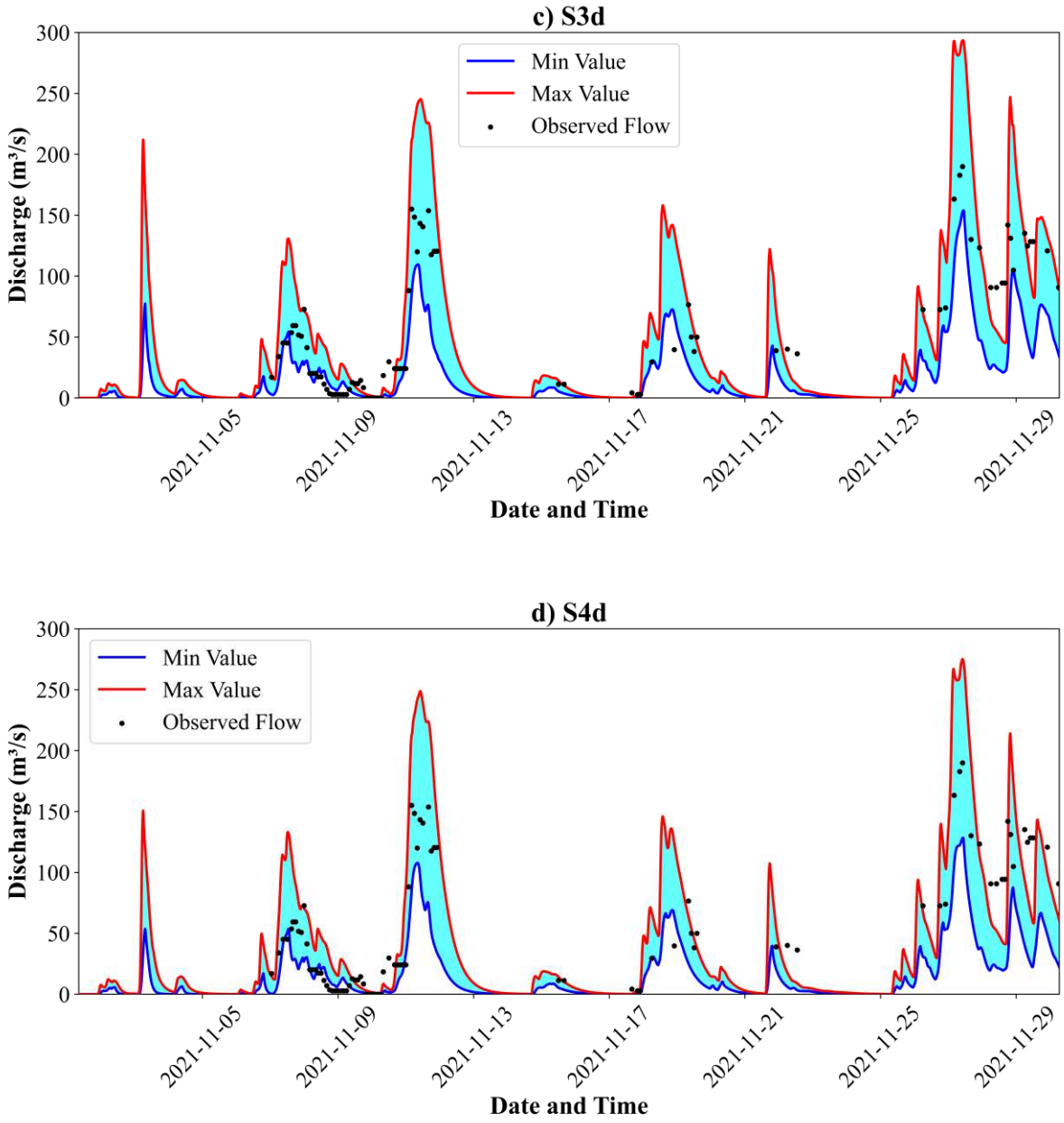


Figure 11. Comparison of simulated ensemble hydrograph with observed hydrographs for the various configurations

The best simulation of the hydrograph for each of the configurations was extracted and plotted as a time series in Figure 12. When the SMRs are not represented in S1, the NSE value for the best simulation was 0.488. This value improves when all the SMRs are represented in S4d to 0.726. From Figure 12, it is visually evident that, for S1, the initial hydrograph is higher than for all other configurations due to the absence of SMR representation. The NSE value for the

best simulation is less than 0.5 when SMRs are only represented as “surface storage” (lumped depression storage). In contrast, when the COS are represented as “reservoirs”, the NSE value for the best simulation exceeds 0.7. The NSE value for the best simulation increased from 0.452 for S2 to 0.786 for S3d. This is due to the watershed response, as reflected in the lag in the hydrograph, which helps to capture the recession limb of the hydrograph better in S3d and S4d than in S1 and S2.

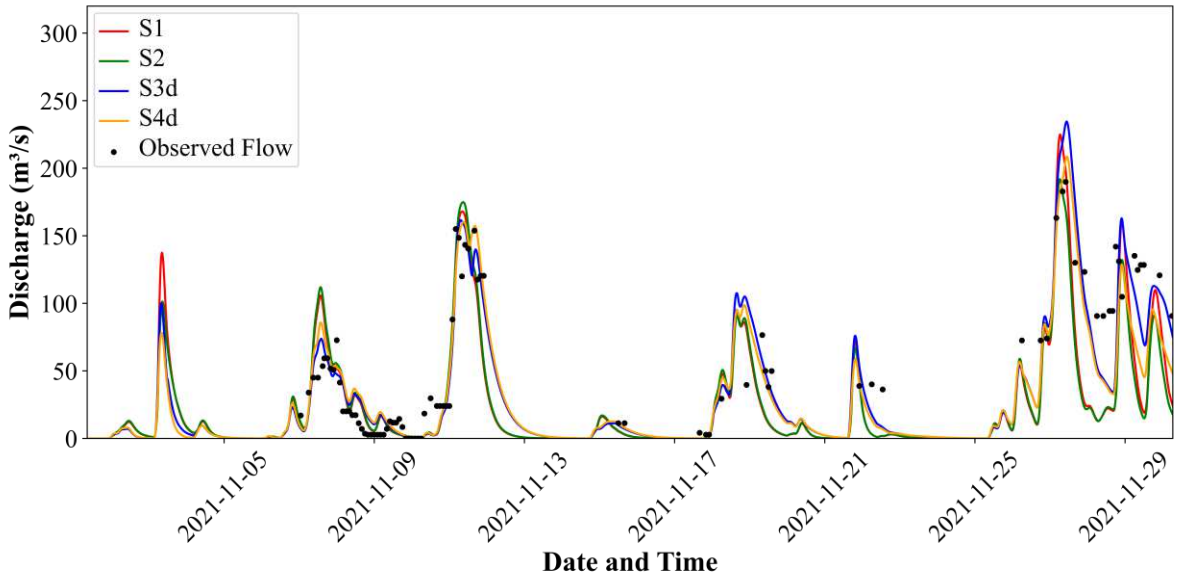


Figure 12. Calibration of the hydrological model for the various configurations

4.5 Validation of the hydrological model

Based on the best-calibrated parameters, validation was performed for NEM 2023. The comparison of the observed and simulated hydrographs is presented in Figure 13. The results of the NEM 2023 showed that the NSE values for S3d (0.56) and S4d (0.58) are better than those for S1 (0.39) and S2 (0.45). In addition, the RMSE values are also lesser for S3d and S4d. Thus, representing COS as “reservoirs” improved the hydrologic model performance during validation. The peak flow is captured better in S3d and S4d when compared to S1 and S2. On the whole, the results demonstrated improved performance of configurations S3d and

S4d when compared to configurations S1 and S2, both during the calibration and validation phases.

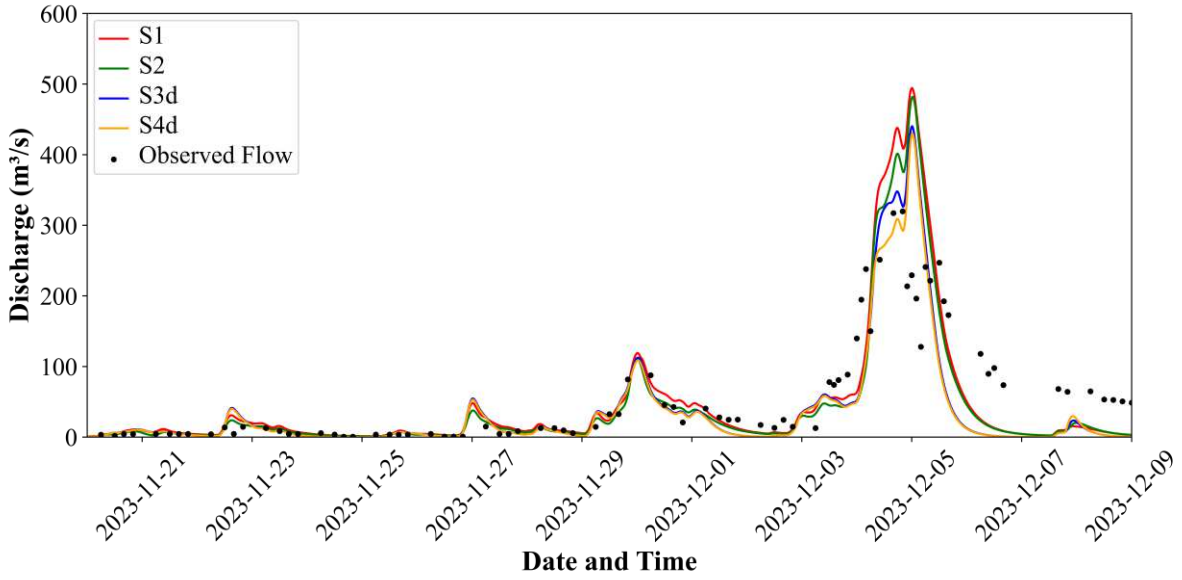


Figure 13. Validation of the hydrological model for the various configurations

Table 2. Variation of the performance metrics for the four configurations - validation

Model Configuration	**S1**	**S2**	**S3d**	**S4d**
NSE	0.39	0.45	0.56	0.58
RMSE (m^3/s)	52.9	50.37	42.27	41.15

4.6 Discussion

This research evaluates the incorporation of small and medium reservoirs (SMRs) into hydrological models such as HEC-HMS, for continuous simulations. Four different model configurations – S1, S2, S3, and S4 were evaluated based on the representation of SMRs in the hydrologic model. A methodology is developed to quantify the model structure and parameter uncertainty associated with the spatial and lumped representation of SMRs in hydrological models for flood simulations.

HEC-HMS offers two methods—"surface storage" and "reservoir" — for representing SMRs. The former is the lumped depression storage, and the latter is the spatially explicit storage. Due to the increasing model structure complexity involved with the representation of all SMRs as reservoirs and the non-availability of Elevation-Area-Capacity (EAC) relationship for all the SMRs (input required in the hydrologic model), this study employs a "hybrid approach" suggested by Habets et al., (2018). The approach incorporated in model configuration S4 combines the lumped depression storage approach for cascade SMRs (CAS) with the spatially explicit approach for catchment outlet SMRs (COS). In modeling COS as reservoirs, the reservoir's initial storage before the simulation is significant. In this regard, the impact of initial storage in the reservoir (0%, 25%, 50%, 75%) on the calibration process for the continuous model simulations was evaluated for S3 and S4 configurations.

The sensitivity analysis was carried out for S1, S2, S3, and S4 configurations independently by considering peak inflow and inflow volume as criteria for comparison. Overall, the impervious percentage was found to be the most sensitive parameter. This finding is in agreement with the sensitivity analysis results from Ouédraogo et al., (2018) for 230 km^2 of the Mkurumudzi River basin using the SMA method, in which the runoff peak was very sensitive to the impervious percentage. The results of the sensitivity analysis showed that, for S1 and S3, the soil parameters were sensitive to both peak inflow and inflow volume. This is because in both S1 and S3, CAS are not represented as "surface storage", whereas in S2 and S4, they are represented. As a result, the surface storage dominates over the soil parameters in S2 and S4. Hence, the soil parameters are not sensitive in S2 and S4 configurations.

NSE, $R^{2,}$ and RMSE are used as performance metrics for comparing observed and simulated hydrographs. The threshold for classifying model performance based on the metrics is highly subjective in nature. In this regard, Pandit et al., (2025) provided the threshold for the metrics for the classification of the model performance, especially for sub-daily flows. NSE > 0.5 is

usually considered for the calibration of the model. However, in this study, the maximum NSE achieved for the S1 and S2 configurations was less than 0.5. Hence, the NSE threshold was reduced from 0.5 to 0.4 to cater to the comparison across configurations. For the continuous simulation, the maximum NSE values for S3d and S4d during calibration of the model are in the 0.7 to 0.8 range, indicating "good" performance. The representation of COS as "reservoirs" improved the performance to the "good" category for S3 and S4 configurations from the "limited" category and the "satisfactory" category for S1 and S2 during the calibration and validation phases, respectively. This result assumes significance as some of the flood mitigation studies have represented the SMRs as "lumped storages" (Devi et al. 2020).

The model structure uncertainty associated with the representation of SMRs has been studied previously (Rabelo et al. 2021; Colombo et al. 2024). However, this study focuses on the quantification of the model structure and parameter uncertainty in the representation of SMRs for flood simulations using variance decomposition. The results demonstrate that the representation of SMRs alone does not increase the model structure uncertainty, as parameter uncertainty dominates model structure uncertainty when S1 and S2 configurations are compared. Similar results are observed when S3d and S4d configurations are compared. For the comparison of the rest of the configurations, it can be understood that the representation of COS as "reservoirs" results in model structure uncertainty dominating parameter uncertainty, irrespective of the increase in NSE value.

As presented in Figure 11a, the S1 configuration led to an overestimation of inflows. The results from the current study agree with the findings of Ramabrahmam et al., (2021), in which the simulation without the SMRs led to the overestimation of the peak inflow as well as the inflow volume. The results from the current study indicate that the performance of S3 (representing the COS alone as "reservoirs") is almost similar to that of S4 (representing the COS as "reservoirs" and CAS as "surface storage"). This agrees with the findings of Rabelo et al.,

(2021), which suggests that the performance of the model for the representation of strategic SMRs was comparable to that of the configuration representing both the strategic SMRs and small reservoirs. Finally, this study reiterates the importance of appropriately representing SMRs in hydrological models for flood simulations that will, in turn, help in the better evaluation of flood mitigation studies.

5. Conclusion

The model structure uncertainty associated with representing SMRs as lumped storages (surface storages) and spatially explicit elements (reservoirs) has been evaluated using the HEC-HMS model for the Chembarambakkam catchment in this study. The methodology involved the conceptualization of the four configurations – S1, S2, S3, and S4 for the various representations of SMRs, followed by the sensitivity analysis and hydrologic model performance evaluation by calibration and validation of the model.

The sensitivity analysis results show that the impervious parameter is the most sensitive parameter to inflow volume based on the sensitivity index (I) value for all configurations and for configurations S2, S3, and S4 when sensitivity is considered for peak flow. Due to the representation of SMRs as lumped depression storage (surface storage) in S2 and S4, the soil parameters, such as soil maximum infiltration, soil storage capacity, and soil tension capacity, are not sensitive to both inflow volume and peak flow. The hydrological modeling results suggest that model configuration S1 (which does not incorporate SMRs) and S2 (which incorporates all SMRs as lumped storage) do not perform satisfactorily. The incorporation of the COS alone as “reservoirs” in HEC-HMS in S3 configuration results in significant improvement in hydrologic model performance when compared to S1 and S2, both during calibration and validation. The configuration S4, which is a combination of S2 and S3, also performs better than S1 and S2. The configurations S3 and S4 captured both the peak and the

recession limb of the observed hydrograph better than S1 and S2. This is mainly because of the incorporation of COS as “reservoirs” in the model configurations of S3 and S4.

This representation of COS as “reservoirs” increased the model structure uncertainty as demonstrated in the variance decomposition analysis. The lumped representation (S2) contributed to the increase in parametric uncertainty. However, when all four configurations were considered, the proportion of model variance dominated the parametric variance. In addition, the representation of COS as “reservoirs” ensured an increase in the p-factor from 0.078 for S1 to 0.449 for S3. Thus, this study emphasizes the importance of appropriately representing SMRs in the hydrological models to improve the performance and reduce the uncertainty for flood simulations.

Declarations

Ethical Approval Not applicable.

Consent to Participate Not applicable.

Consent to Publish

The authors declare their consent of the publication of this manuscript by “Water Resources Management” journal.

Author Contributions

Conceptualization: Elanchezhiyan Duraisekaran, Krushil Modi, Arun Rajasekaran Sankarbalaji; Methodology: Elanchezhiyan Duraisekaran, Krushil Modi, Arun Rajasekaran Sankarbalaji, ; Formal analysis and investigation: Elanchezhiyan Duraisekaran; Writing - original draft preparation: Elanchezhiyan Duraisekaran; Writing - review and editing: Elanchezhiyan Duraisekaran, Balaji Narasimhan, Arun Rajasekaran Sankarbalaji; Funding

acquisition: Balaji Narasimhan; Resources: Balaji Narasimhan; Supervision: Balaji Narasimhan.

Funding

This work was funded by the Department of Science and Technology, Ministry of Science and Technology, Grant/Award Number: DST/CCP/CoE/141/2018(G).

Competing Interests

The authors declare no conflict of interest.

Availability of Data and Materials

Datasets are available upon request.

References

Abbaspour KC (2015) SWAT calibration and uncertainty programs

Azmat M, Qamar MU, Ahmed S, et al (2017) Application of HEC-HMS for the event and continuous simulation in high-altitude scarcely-gauged catchment under changing climate. Eur Water 57:77–84

Bhavsar PN, Patel JN (2020) Event-based rainfall–run-off modeling and uncertainty analysis for lower Tapi Basin, India. ISH J Hydraul Eng 26:353–362. https://doi.org/10.1080/09715010.2018.1464406

Boulange J, Hanasaki N, Yamazaki D, Pokhrel Y (2021) Role of dams in reducing global flood exposure under climate change. Nat Commun 12:1–7. https://doi.org/10.1038/s41467-020-20704-0

Brunner MI (2021) Reservoir regulation affects droughts and floods at local and regional scales. Environ Res Lett 16:. https://doi.org/10.1088/1748-9326/ac36f6

Colombo P, Ribeiro Neto GG, Costa AC, et al (2024) Modeling the influence of small reservoirs on hydrological drought propagation in space and time. J Hydrol 629:130640. https://doi.org/10.1016/j.jhydrol.2024.130640

Datta AR, Bolisetti T (2013) Application of variance decomposition approach in the uncertainty analysis of a hydrological model. Can J Civ Eng 40:373–381. https://doi.org/10.1139/cjce-2012-0337

Devi NN, Sridharan B, Bindhu VM, et al (2020) Investigation of role of retention storage in tanks (Small water bodies) on future urban flooding: A case study of chennai city, india. Water (Switzerland) 12:1–30. https://doi.org/10.3390/w12102875

Donchyts G, Winsemius H, Baart F, et al (2022) High-resolution surface water dynamics in Earth's small and medium-sized reservoirs. Sci Rep 12:13776

Duan Y, Xiong J, Cheng W, et al (2022) Assessment and spatiotemporal analysis of global flood vulnerability in 2005–2020. Int J Disaster Risk Reduct 80:103201. https://doi.org/10.1016/j.ijdrr.2022.103201

Fleming M, Neary V (2004) Continuous Hydrologic Modeling Study with the Hydrologic Modeling System. J Hydrol Eng 9:175–183. https://doi.org/10.1061/(asce)1084-0699(2004)9:3(175)

Gupta A, Govindaraju RS (2023) Uncertainty quantification in watershed hydrology: Which method to use? J Hydrol 616:128749. https://doi.org/10.1016/j.jhydrol.2022.128749

Habets F, Molénat J, Carluer N, et al (2018) The cumulative impacts of small reservoirs on hydrology: A review. Sci Total Environ 643:850–867. https://doi.org/10.1016/j.scitotenv.2018.06.188

Han B, Zhang Y, Shao Q, et al (2025) Estimating multi-source input uncertainties and their

propagation for integrated water quantity and quality simulations. Hydrol Sci J 70:2976–2992. https://doi.org/10.1080/02626667.2025.2570849

Han D, Liu P, Zhang L, et al (2024) Quantifying the impact of dams on global streamflow over the period of 1985-2014. Environ Res Lett 19:. https://doi.org/10.1088/1748-9326/ad6a70

Hanazaki R, Yamazaki D, Yoshimura K (2022) Development of a Reservoir Flood Control Scheme for Global Flood Models. J Adv Model Earth Syst 14:. https://doi.org/10.1029/2021MS002944

Holberg J (2014) Tutorial on using HEC-GeoHMS to develop soil moisture accounting method inputs for HEC-HMS. Purdue Univ West Lafayette, IN, USA

Lenhart T, Eckhardt K, Fohrer N, Frede H. (2002) Comparison of two different approaches of sensitivity analysis. Phys Chem Earth, Parts A/B/C 87:645–654. https://doi.org/10.1007/BF01743071

Ma Q, Xiong L, Liu D, et al (2018) Evaluating the temporal dynamics of uncertainty contribution from satellite precipitation input in rainfall-runoff modeling using the variance decomposition method. Remote Sens 10:1–25. https://doi.org/10.3390/rs10121876

Mahmoodi N, Wagner PD, Lei C, et al (2024) Enhancing hydrologic modelling through the representation of traditional rainwater harvesting systems: A case study of water tanks in South India. Hydrol Process 38:1–11. https://doi.org/10.1002/hyp.15088

McKay MD, Beckman RJ, Conover WJ (2000) A comparison of three methods for selecting values of input variables in the analysis of output from a computer code. Technometrics 42:55–61. https://doi.org/10.1080/00401706.2000.10485979

Mousavi SJ, Kamali B, Abbaspour KC, et al (2012) Uncertainty-based automatic calibration of HEC-HMS model using sequential uncertainty fitting approach. J Hydroinformatics 14:286–309. https://doi.org/10.2166/hydro.2011.071

Núñez Mejía SX, Mendoza Paz S, Tabari H, Willems P (2023) Climate change impacts on hydrometeorological and river hydrological extremes in Quito, Ecuador. J Hydrol Reg Stud 49:1–20. https://doi.org/10.1016/j.ejrh.2023.101522

Odey G, Cho Y (2025) Event-Based vs. Continuous Hydrological Modeling with HEC-HMS: A Review of Use Cases, Methodologies, and Performance Metrics. Hydrology 12:. https://doi.org/10.3390/hydrology12020039

Ouédraogo WAA, Raude JM, Gathenya JM (2018) Continuous modeling of the Mkurumudzi River catchment in Kenya using the HEC-HMS conceptual model: Calibration, validation, model performance evaluation and sensitivity analysis. Hydrology 5:. https://doi.org/10.3390/hydrology5030044

Pandit A, Hogan S, Mahoney DT, et al (2025) Establishing performance criteria for evaluating watershed-scale sediment and nutrient models at fine temporal scales. Water Res 274:123156. https://doi.org/10.1016/j.watres.2025.123156

Pappenberger F, Harvey H, Beven K, et al (2006) Decision tree for choosing an uncertainty analysis methodology: a wiki experiment. Hydrol Process 20:3793–3798. https://doi.org/10.1002/hyp

Perera KTN, Wijayaratna TMN, Jayatillake HM, et al (2020) Hydrological principle behind the development of series of bunds in ancient tank cascades in small catchments, sri lanka. Water Pract Technol 15:1174–1189. https://doi.org/10.2166/wpt.2020.088

Pi X, Luo Q, Feng L, et al (2022) Mapping global lake dynamics reveals the emerging roles

of small lakes. Nat Commun 13:1–12. https://doi.org/10.1038/s41467-022-33239-3

Rabelo UP, Costa AC, Dietrich J, et al (2022) Impact of Dense Networks of Reservoirs on Streamflows at Dryland Catchments. Sustain 14:. https://doi.org/10.3390/su142114117

Rabelo UP, Dietrich J, Costa AC, et al (2021) Representing a dense network of ponds and reservoirs in a semi-distributed dryland catchment model. J Hydrol 603:. https://doi.org/10.1016/j.jhydrol.2021.127103

Ramabrahmam K, Keesara VR, Srinivasan R, et al (2021) Flow simulation and storage assessment in an ungauged irrigation tank cascade system using the SWAT model. Sustain 13:. https://doi.org/10.3390/su132313158

Sahu MK, Shwetha HR, Dwarakish GS (2023) State-of-the-art hydrological models and application of the HEC-HMS model: a review. Model Earth Syst Environ 9:3029–3051. https://doi.org/10.1007/s40808-023-01704-7

Sankarbalaji AR, Duraisekaran E, Sangeetha K, et al (2025) Assessment of increasing hydrologic model complexity in the representation of small and medium reservoirs within a river basin scale model and its impact on process simulation and parameter uncertainty. J Hydrol 655:132925. https://doi.org/10.1016/j.jhydrol.2025.132925

Spinti RA, Condon LE, Zhang J (2023) The evolution of dam induced river fragmentation in the United States. Nat Commun 14:1–9. https://doi.org/10.1038/s41467-023-39194-x

Stein M (1987) Large sample properties of simulations using latin hypercube sampling. Technometrics 29:143–151. https://doi.org/10.1080/00401706.1987.10488205

Sun J, Chen W, Hu B, et al (2023) Roles of reservoirs in regulating basin flood and droughts risks under climate change: Historical assessment and future projection. J Hydrol Reg Stud 48:101453. https://doi.org/10.1016/j.ejrh.2023.101453

USACE (2025) Hydrologic Modeling System HEC-HMS Technical Reference Manual

Xu Y, Yan B (2022) Quantifying interaction uncertainty between subwatersheds and base-flow partitions on hydrological processes. PLoS One 17:1–22. https://doi.org/10.1371/journal.pone.0261859

Yan X, Lin B, Chen X, et al (2023) Impacts of small and medium-sized reservoirs on streamflow in two basins of Southeast China, using a hydrological model to separate influences of multiple drivers. J Hydrol Reg Stud 50:101582. https://doi.org/10.1016/j.ejrh.2023.101582

Yip S, Ferro CAT, Stephenson DB, Hawkins E (2011) A Simple, coherent framework for partitioning uncertainty in climate predictions. J Clim 24:4634–4643. https://doi.org/10.1175/2011JCLI4085.1